

A Knowledge Compilation Map for Quantum Information

Lieuwe Vinkhuijzen, Tim Coopmans, Alfons Laarman

Leiden University, The Netherlands

Abstract

Quantum computing is finding promising applications in optimization, machine learning and physics, leading to the development of various models for representing quantum information. Because these representations are often studied in different contexts (many-body physics, machine learning, formal verification, simulation), little is known about fundamental trade-offs between their succinctness and the runtime of operations to update them. We therefore analytically investigate three widely-used quantum state representations: matrix product states (MPS), decision diagrams (DDs), and restricted Boltzmann machines (RBMs). We map the relative succinctness of these data structures and provide the complexity for relevant query and manipulation operations. Further, to chart the balance between succinctness and operation efficiency, we extend the concept of rapidity with support for the non-canonical data structures studied in this work, showing in particular that MPS is at least as rapid as some DDs.

By providing a knowledge compilation map for quantum state representations, this paper contributes to the understanding of the inherent time and space efficiency trade-offs in this area.

1 Introduction

Quantum computers promise large computational advantages compared to classical computers in areas ranging from mathematics to chemistry. To support this development, various classical methods have been proposed to analyze quantum systems. A major bottleneck is that the state of a quantum system is described by an exponential-sized amplitude vector, and it is difficult to represent this object in general. Therefore, different disciplines, from physics to computer science, have come up with data structures that enable quantum state representation and manipulation: in order to simulate, verify and analyze new quantum algorithms, (algebraic) decision diagrams (DDs) have been proposed (Miller and Thornton 2006; Viamontes, Markov, and Hayes 2003). To study physical quantum systems, physicists have developed tensor networks (TNs; (Schollwöck 2011)), matrix product states (MPS; (Orús 2014), sometimes also called tensor trains) —a specialization of TNs—, and restricted Boltzmann machines (RBMs; (Dumoulin et al. 2014)) with complex values, a specialization of Neural Quantum States (Carleo and Troyer 2017). Recently these methods have

been growing towards each other, for instance, with the development of quantum circuit simulation for MPS (Vidal 2003), combinations of TNs and DDs (Hong et al. 2022), MPS and decision diagrams (Burgholzer, Ploier, and Wille 2023), a comparison between TNs and probabilistic graphical models (Glasser et al. 2019), and the extension of DDs with support for stabilizer states, yielding so-called LIMDDs (Vinkhuijzen et al. 2023a).

However, fundamental differences between these data structures have not yet been studied in detail. This choice between different structures introduces an important trade-off between *size* and *speed*, i.e., how much space the data structure uses, versus how fast certain operations, such as measurement, can be performed. This trade-off plays a crucial role in other areas as well, and has already been illuminated for the domain of explainable AI (Audemard, Koriche, and Marquis 2020) and logic (Darwiche and Marquis 2002; Fargier et al. 2014), but not yet for quantum information.

In this work, we analytically compare for the first time several data structures for representing and manipulating quantum states, motivated by the following three applications. First, *simulating quantum circuits*, the building block of quantum computations, is a crucial tool for predicting the performance and scaling behavior of experimental devices with various error sources, thereby guiding hardware development (Zulehner and Wille 2018; Thanos et al. 2023). Next, *variational methods* are the core of *quantum machine learning* (Benedetti et al. 2019; Dunjko and Briegel 2017) and solve quantum physics questions such as finding the lowest energy of a system of quantum particles (Foulkes et al. 2001; Carleo and Troyer 2017). Finally, *verifying* if two quantum circuits are equivalent is crucial for checking if a (synthesized or optimized) quantum circuit satisfies its specification (Ardeshir-Larijani, Gay, and Nagarajan 2014; Gay and Nagarajan 2005; Burgholzer and Wille 2020).

We focus on data structures developed for the above applications. In particular, we focus on: algebraic decision diagrams (ADD), semiring-labeled decision diagrams (SLDD_×, also called QMDD), local invertible map decision diagrams (LIMDD), matrix product states (MPS) and restricted Boltzmann machines (RBM). For those, we study *succinctness*, *tractability* and *rapidity*:

Succinctness & Tractability. In Sec. 3, we find that the succinctness of MPS, RBM and LIMDD are incomparable. We also find that MPS is strictly more succinct than SLDD_\times , whereas previous research had suggested that these were incomparable (Burgholzer, Ploier, and Wille 2023). In Sec. 4, we give states which SLDD_\times and LIMDD can compactly represent, but which take exponential time to apply Hadamard and swap gates. Finally, we prove that computing fidelity and inner product in RBM and LIMDD is intractable assuming the exponential time hypothesis. An operation on a data structure is said to be *tractable* if it runs in polynomial time in the size of the input (Darwiche and Marquis 2002).

Rapidity. Considering tractability and succinctness separately can deceive; for instance, when representing a quantum state as an amplitude vector, most operations (e.g., applying a single-qubit gate) are polynomial time in the size of the size of this vector; thus, these exponential-time operations would be called tractable. Of course, this is only because this vector has exponential size in the number of qubits. To mend this deficiency, (Lai, Liu, and Yin 2017) introduced the notion of *rapidity*, which reflects the idea that exponential operations may be preferable if a representation can be exponentially more succinct.

In Sec. 5, we generalize the definition of rapidity for non-canonical data structures, which allows us to study rapidity of MPS and RBM. We also give a simple sufficient condition for data structures to be more rapid than others (for all operations). We use it to settle several rapidity relations, showing surprisingly that MPS is strictly more rapid than SLDD_\times . Since we are unaware of a previous comparison, our knowledge was consistent with them being incomparable.

Proofs of all claims are provided in the appendix.

2 Data Structures for Quantum States

2.1 Quantum Information

To understand our main results, it suffices to know the following (we refer to App. A and (Nielsen and Chuang 2000) for a more elaborate treatment of quantum information and computing). A quantum state φ on n quantum bits or qubits,

written in Dirac notation as $|\varphi\rangle$, can be represented as a vector of 2^n complex *amplitudes* $a_k \in \mathbb{C}$ such that the vector has unit norm, i.e. $\sum_{k=1}^{2^n} |a_k|^2 = 1$, where $|z| = \sqrt{a^2 + b^2}$ is the modulus of a complex number $z = a + b \cdot i$ with $a, b \in \mathbb{R}$. We also write $a_k = \langle k|\varphi\rangle$. Two quantum states $|\varphi\rangle, |\psi\rangle$ are equivalent if $|\varphi\rangle = \lambda|\psi\rangle$ for some complex λ . The inner product between two quantum states $|\varphi\rangle, |\psi\rangle$ is $\langle\varphi|\psi\rangle = \sum_{k=1}^{2^n} (\langle k|\varphi\rangle)^* \cdot \langle k|\psi\rangle$ where $z^* = a - bi$ is the complex conjugate of the complex number $z = a + b \cdot i$. The fidelity $|\langle\varphi|\psi\rangle|^2 \in [0, 1]$ is a measure of closeness, with fidelity equalling 1 if and only if $|\varphi\rangle$ and $|\psi\rangle$ are equivalent.

A quantum circuit consists of gates and measurements. An n -qubit *gate* is a $2^n \times 2^n$ unitary matrix which updates the n -qubit state vector by matrix-vector multiplication. A k -local gate is a gate which effectively only acts on a subregister of $k \leq n$ qubits. Often-used gates go by names Hadamard (H), T , Swap, and the Pauli gates X, Y, Z . Together with the two-qubit gate controlled- Z , the H and T gate form a universal gate set (i.e. any quantum gate can be arbitrarily well approximated by circuits of these gates only). Next, a (computational-basis) measurement is an operation which samples n bits from (a probability distribution defined by) the quantum state, *while also updating the state*.

We now elaborate on the application domains from Sec. 1. *Simulating a circuit* using the data structures in this work starts wlog by constructing a data structure for some (simple) initial state $|\varphi_0\rangle$, followed by manipulating the data structure by applying the gates and measurements A, B, \dots of the circuit one by one, i.e.: $|\varphi_1\rangle = A|\varphi_0\rangle, |\varphi_2\rangle = B|\varphi_1\rangle$, etc. The data structure supports strong (weak) simulation, if, for each measurement gate, it can produce (a sample of) the probability function (as a side result of the state update). Next, the quantum circuit of *variational methods* consist of a quantum circuit; then the output state $|\varphi\rangle$ is used to compute $\langle\varphi|O|\varphi\rangle$ for some linear operator O (an *observable*). This computation reduces to $\langle\varphi|\psi\rangle$ with $|\psi\rangle := O|\varphi\rangle$ (i.e., computing simulation and fidelity). Last, *circuit verification* relies on checking approximate or exact equivalence of quantum states. This extends to unitary matrices (gates), which all data structures from this paper can represent also, but which we will not treat for simplicity.

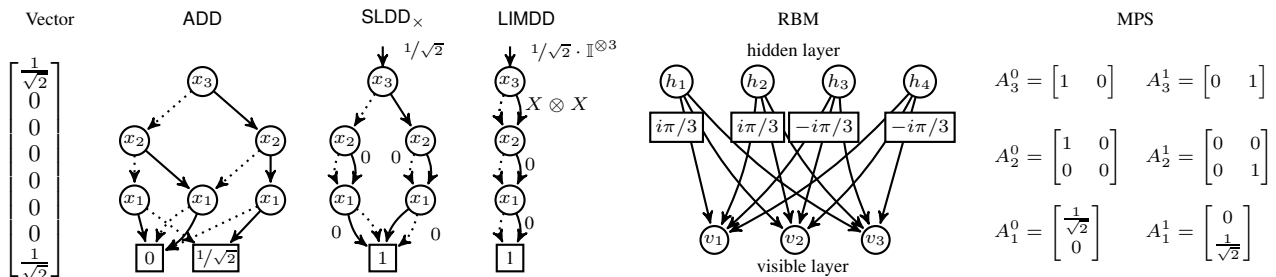


Figure 1: The 3-qubit GHZ state $\frac{1}{\sqrt{2}}(|000\rangle + |111\rangle)$, displayed using different data structures. The unlabelled edges for ADD, SLDD_\times , LIMDD have resp. label 1, 1, \mathbb{I} . In the RBM, the weights of edges incident to h_1, h_2 (h_3, h_4) are all $i\pi/3$ ($-i\pi/3$); the hidden node biases $(\beta_{h_1}, \beta_{h_2}, \beta_{h_3}, \beta_{h_4}) = i\pi \cdot (1/3, 2/3, -1/3, -2/3)$; the visible node biases $\alpha_{v_1} = \alpha_{v_2} = \alpha_{v_3} = 0$.

2.2 Data Structures

We now define the data structures for representing quantum states considered in this work, with examples in Fig. 1.

Definition 1 (Inspired by (Fargier et al. 2014)). A *quantum-state representation (language)* is a tuple $(D, n, |\cdot\rangle, |\cdot|)$ where D is a set of data structures. Given $\alpha \in D$, $|\alpha\rangle$ is the (possibly unnormalized) quantum state it represents (i.e., the interpretation of α), $|\alpha|$ is the size of the data structure, and $n(\alpha)$, or n in short, is the number of qubits of $|\alpha\rangle$. Finally, each quantum state should be expressible in the language.

We will often refer to a representation as a data structure. We define $D^\varphi \triangleq \{\alpha \in D \mid |\alpha\rangle = |\varphi\rangle\}$, i.e., the set of all data structures in language D representing state $|\varphi\rangle$. In line with quantum information, we say that data structures α, β are *equivalent* if $|\alpha\rangle = \lambda |\beta\rangle$ for some $\lambda \in \mathbb{C}$.

Vector. A state vector α is a length- 2^n array of complex entries $a_k \in \mathbb{C}^{2^n}$ satisfying $\sum_{k=1}^{2^n} |a_k|^2 = 1$, and interpretation $|\alpha\rangle = \sum_j \alpha_j |j\rangle$. Despite its size, the vector representation is used in many simulators (Jones et al. 2019). We mainly include the vector representation to show that considering operation tractability alone can be deceiving.

Matrix Product States (MPS). An MPS M is a series of $2n$ matrices $A_k^x \in \mathbb{C}^{D_k \times D_{k-1}}$ where $x \in \{0, 1\}$, $k \in [n]$ and D_k is the row dimension of the k -th matrix with $D_0 = D_n = 1$. The interpretation $|M\rangle$ is determined as $\langle \vec{y} | M \rangle = A_n^{x_n} \cdots A_2^{x_2} A_1^{x_1}$ for $\vec{y} \in \{0, 1\}^n$. The size of M is the total number of matrix elements, i.e., $|M| = 2 \cdot \sum_{k=1}^n D_k \cdot D_{k-1}$. We will speak of $\max_{j \in [0 \dots n]} D_j$ as ‘the’ bond dimension.

Restricted Boltzmann Machine (RBM). An n -qubit RBM is a tuple $\mathcal{M} = (\vec{\alpha}, \vec{\beta}, W, m)$, where $\vec{\alpha} \in \mathbb{C}^n, \vec{\beta} \in \mathbb{C}^m$ for $m \in \mathbb{N}_+$ are *bias vectors* and $W \in \mathbb{C}^{n \times m}$ is a *weight matrix*. An RBM \mathcal{M} represents the state $|\mathcal{M}\rangle$ as follows.

$$\langle \vec{x} | \mathcal{M} \rangle = e^{\vec{x}^T \cdot \vec{\alpha}} \cdot \prod_{j=1}^m (1 + e^{\beta_j + \vec{x}^T \cdot \vec{W}_j}) \quad (1)$$

where \vec{W}_j is the j -th column of W , β_j is the j -th entry of $\vec{\beta}$ and where we write $\vec{x}^T \cdot \vec{W}_j$ to denote the inner product of the row vector \vec{x}^T and the column vector \vec{W}_j (Chen et al. 2018). The size of \mathcal{M} is $|\mathcal{M}| = n + m + n \cdot m$. We say this RBM has n *visible nodes* and m *hidden nodes*. A weight $W_{v,j}$ is an edge from the v -th visible node to the j -th hidden node. The j -th hidden node is said to contribute the multiplicative term $(1 + e^{\beta_j + \vec{x}^T \cdot \vec{W}_j})$.

Quantum Decision Diagrams (QDD). We define a Quantum Decision Diagram to represent a quantum state, based on the Valued Decision Diagram (Fargier et al. 2014) as instantiated on a domain of binary variables (qubits) and a co-domain of complex values (amplitudes). A QDD α is a finite, rooted, directed acyclic graph (V, E) , where each node v is labeled with an index $\text{idx}(v) \in [n]$ and leaves

Table 1: Various decision diagrams treated by the literature. The column *Merging strategy* lists the conditions under which two nodes v, w , representing subfunctions $f, g: \{0, 1\}^k \rightarrow \mathbb{C}$ are merged. Here $p, a \in \mathbb{C}$ are complex constants, P_i are Pauli gates and $f + a$ means the function $f(\vec{x}) + a$ for all \vec{x} . We list SLDD₊ and AADD for completeness, but do not consider them.

(Quantum) decision diagrams (and variants)	Node merging strategy
Decision Tree	(no merging)
ADD (Bahar et al. 1997), MTBDD (Clarke et al. 1993), QuiDD (Viamontes, Markov, and Hayes 2003)	$f = g$
SLDD _× (Wilson 2005; Fargier, Marquis, and Schmidt 2013), QMDD (Miller and Thornton 2006)	$f = p \cdot g$
SLDD ₊ (Fargier, Marquis, and Schmidt 2013), EVBDD (Lai, Pedram, and Vrudhula 1994)	$f = g + a$
AADD (Sanner and McAllester 2005), FEVBDD (Tafertshofer and Pedram 1997)	$f = p \cdot g + a$
LIMDD (Vinkhuijzen et al. 2023a)	$f = pP_1 \otimes \dots \otimes P_n \cdot g$

have index 0. In addition, a ‘root edge’ e_R (without a source node) points to the root node. Each node has two outgoing edges, one labeled 0 (the low edge) and one labeled 1 (the high edge). In addition, edge $e = vw$ pointing to a node w with index k has a label $\text{label}(e) \in \mathcal{E}_k$ for some edge label set \mathcal{E}_k ; in this paper, \mathcal{E}_k is a group (for SLDD_× and LIMDD below with 0 added). Also, each leaf node v has a label $\text{label}(v) \in \mathcal{L}$. The size of a QDD is $|\alpha| = |V| + |E| + \sum_{v \in V} |\text{label}(v)| + \sum_{e \in E \cup \{e_R\}} |\text{label}(e)|$. For simplicity, we require that no nodes are skipped, i.e. $\forall vw \in E: \text{id}[v] = \text{id}[w] + 1$.^{*} The semantics are:

- A leaf node v represents the value $\text{label}(v)$.
- A non-leaf node $\bigcirc \xrightarrow{e_{low}} \bigcirc \xrightarrow{e_{high}} \bigcirc$ represents $|v\rangle = |0\rangle \otimes |e_{low}\rangle + |1\rangle \otimes |e_{high}\rangle$.
- An edge $\xrightarrow{e} \bigcirc$ represents $|e\rangle = \text{label}(e) \cdot |v\rangle$.

Consequently, any node v at level k , i.e., with $\text{idx}(v) = k$, is k edges away from a leaf (along all paths) and therefore represents a k -qubit quantum state (or a complex vector).

In this paper, we consider the following types of QDDs. We emphasize that an ADD can be seen as a special case of SLDD_×, which is a special case of LIMDD.

ADD: $\forall k: \mathcal{E}_k = \{1\}, \mathcal{L} = \mathbb{C}$ (Bahar et al. 1997).

SLDD_×: $\forall k: \mathcal{E}_k = \mathbb{C}, \mathcal{L} = \{1\}$ (Wilson 2005).

LIMDD: $\forall k: \mathcal{E}_k = \text{PAULILIM}_k \cup \{0\}, \mathcal{L} = \{1\}$, where $\text{PAULILIM}_k \triangleq \{\lambda P \mid \lambda \in \mathbb{C} \setminus \{0\}, P \in \{\mathbb{I}, X, Y, Z\}^{\otimes k}\}$, i.e., the group generated by k -fold tensor products of the single-qubit Pauli matrices (Vinkhuijzen et al. 2023a):

$$\mathbb{I} \triangleq \begin{pmatrix} 1 & 0 \\ 0 & 1 \end{pmatrix}, X \triangleq \begin{pmatrix} 0 & 1 \\ 1 & 0 \end{pmatrix}, Y \triangleq \begin{pmatrix} 0 & -i \\ i & 0 \end{pmatrix}, Z \triangleq \begin{pmatrix} 1 & 0 \\ 0 & -1 \end{pmatrix}$$

Two isomorphic QDD nodes (Def. 2) v, w with $|w\rangle = \ell |v\rangle$ can be *merged* by removing w and rerouting all edges $uw \in E$

^{*}Asymptotic analysis is not affected by disallowing node skipping as it yields linear-size reductions at best (Knuth 2005).

E incoming to w to v , updating their edge labels accordingly (i.e., $\text{label}(uv) := \text{label}(uw) \cdot \ell$). Table 1 summarizes merging strategy for the above QDDs and related versions. If all isomorphic nodes are merged, we call a QDD *reduced*. We may assume a QDD is reduced (and even canonical), since it can be reduced in polynomial time and manipulation algorithms keep the QDD reduced using a `MAKENODE` operation (Bryant 1986; Miller and Thornton 2006; Fargier, Marquis, and Schmidt 2013; Vinkhuijzen et al. 2023a).

Definition 2 (Isomorphic nodes). QDD node v is isomorphic to node w , if there exists an edge label $\ell \in \mathcal{E}_{\text{idX}(v)}, \ell \neq 0$ such that $\ell \cdot |v\rangle = |w\rangle$. Since $\mathcal{E}_{\text{idX}(v)}$ is a group, $\ell \in \mathcal{E}_{\text{idX}(v)}$ implies $\ell^{-1} \in \mathcal{E}_{\text{idX}(v)}$ so $\ell^{-1} |w\rangle = |v\rangle$. Hence isomorphism is an equivalence relation.

It is well known that the variable order greatly influences QDD sizes (Bollig and Wegener 1996; Darwiche 2011; Bova 2016). Our results here assume any variable order: For instance, when we say that some structure is strictly more succinct than a QDD, it means that there is no variable order for which the QDD is more succinct than the other structure (for representing a certain worst-case state).

3 Succinctness of Quantum Representations

In this section, we compare the succinctness of the data structures introduced in Sec. 2. A language L_1 is as succinct as L_2 if L_2 uses at least as much space to represent any quantum state as L_1 , up to polynomial factors. Thus, a more succinct diagram is more expressive when we constrain ourselves to polynomial (or asymptotically less) space. We define a language L_1 to be *at least as succinct* as L_2 (written $L_1 \preceq_s L_2$), if there exists a polynomial p such that for all $\beta \in L_2$, there exists $\alpha \in L_1$ such that $|\alpha\rangle = |\beta\rangle$ and $|\alpha| \leq p(|\beta|)$. We say that L_1 is more succinct ($L_1 \prec_s L_2$) if L_1 is at least as succinct as L_2 but not vice versa.

The results of this section are summarized by Th. 1 (Fig. 2). We now highlight our novel results. First, we show that MPS \prec_s SLDD $_{\times}$, by (i) describing a simple and efficient way to write a SLDD $_{\times}$ as an MPS, and (ii) finding a fam-

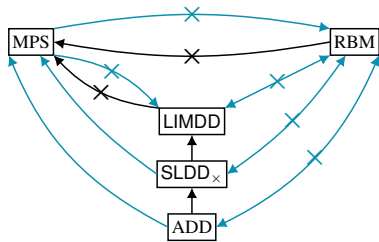


Figure 2: Succinctness relations between various classical data structures for representing quantum states. Solid arrows $A \rightarrow B$ denote $B \prec_s A$, i.e., B is strictly more succinct than A . Crossed arrows $A \not\prec_s B$ denote a separation $B \not\prec_s A$; a bidirectional crossed arrow implies incomparability. Blue arrows indicate novel relations that we identified.

ily of states, which we call $|\text{Sum}\rangle$, which have small MPS but which require exponentially large SLDD $_{\times}$. It follows that MPS \prec_s ADD. Second, we strengthen (ii) to show that the same state also requires exponentially large LIMDDs, thus we establish LIMDD $\not\prec_s$ MPS. The reverse here also holds because MPS cannot efficiently represent certain stabilizer states, while LIMDD is small for all stabilizer states, as shown in (Vinkhuijzen et al. 2023a). Lastly, we show that RBMs can efficiently represent $|\text{Sum}\rangle$. Since it is well-known that RBM explodes for parity functions, which are small for QDD (Martens et al. 2013), we establish incomparability of RBM with all three QDDs.

Theorem 1. The succinctness results in Fig. 2 hold.

4 Tractability of Quantum Operations

In this section, we investigate for each data structure (DS) the tractability of the main relevant queries and manipulation operations for the different applications discussed Sec. 1.

By a *manipulation operation*, we mean a map $D^c \rightarrow D$ and by a *query operation* a map $D^c \rightarrow \mathbb{C}$, where D is a class of data structures and $c \in \mathbb{N}_{\geq 1}$ the number of operands. We say that a class of data structures D *supports* a (query or manipulation) operation $OP(D)$, if there exists an algorithm implementing OP whose runtime is polynomial in the size of the operands, i.e., $|\varphi_1| + \dots + |\varphi_c|$.

The operations whose tractability we investigate are:

- **Sample**: Given a DS representing $|\varphi\rangle$, sample the measurement outcomes $\vec{x} \in \{0, 1\}^n$ from measuring all qubits of $|\varphi\rangle$ in the computational basis.
- **Measure**: Given a DS representing $|\varphi\rangle$ and $\vec{x} \in \{0, 1\}^n$, compute the probability to get \vec{x} when measuring $|\varphi\rangle$.
- **Gates (Hadamard, Pauli X,Y,Z, Controlled-Z CZ, Swap, T)**: Given a DS representing $|\varphi\rangle$ and a one- or two-qubit gate U , construct a DS representing $U|\varphi\rangle$. This gate set is universal (Bravyi and Kitaev 2005) and is used by many algorithms (Vandaele et al. 2023).
- **Local** (Local gates) as general case of Gates: Given a DS representing $|\varphi\rangle$, a constant $k \in \mathbb{N}_{\geq 1}$ and a k -local gate U , construct a DS representing the state $U \cdot |\varphi\rangle$.
- **Addition**: Given DSs for states $|\varphi\rangle, |\psi\rangle$, construct a DS representing the state $|\varphi\rangle + |\psi\rangle$.
- **InnerProd** (inner product) and **Fidelity**: Given DSs for states $|\psi\rangle, |\psi\rangle$, compute $\langle\varphi|\psi\rangle$ and $|\langle\varphi|\psi\rangle|^2$.
- **Equal** (Equality): Decide whether the states represented by two given data structures are equivalent.

We are motivated to study these operations by their applicability in the three application domains from Sec. 1. First, classical simulation of quantum circuits includes **Gates**, as well as **Measure** (strong simulation) and **Sample** (weak simulation). Although **Addition** is not, technically speaking, a quantum operation, we include it because addition of quantum states can happen due to quantum operations. For

Table 2: Tractability of queries and manipulations on the data structures analyzed in this paper (single application of the operation). A \checkmark means the data structure supports the operation in polytime, a \checkmark' means supported in randomized polytime, and \times means the data structure does not support the operation in polytime. A \circ means the operation is not supported in polytime unless $P = NP$. ? means unknown. The table only considers deterministic algorithms (for some ? a probabilistic algorithm exists, e.g., for **InnerProd** on RBM). Novel results are blue and underlined>.

	Queries					Manipulation operations						
	Sample	Measure	Equal	InnerProd	Fidelity	Addition	Hadamard	X,Y,Z	CZ	Swap	Local	T-gate
Vector	\checkmark	\checkmark	\checkmark	\checkmark	\checkmark	\checkmark	\checkmark	\checkmark	\checkmark	\checkmark	\checkmark	\checkmark
ADD	\checkmark	\checkmark	\checkmark	\checkmark	\checkmark	\checkmark	\checkmark	\checkmark	\checkmark	\checkmark	\checkmark	\checkmark
SLDD \times	\checkmark	\checkmark	\checkmark	\checkmark'	\checkmark'	\times	\times	\checkmark'	\checkmark'	\times	\times	\checkmark'
LIMDD	\checkmark	\checkmark	\checkmark	\circ	\circ	\times	\times	\checkmark	\checkmark	\times	\times	\checkmark'
MPS	\checkmark	\checkmark	\checkmark	\checkmark	\checkmark	\checkmark	\checkmark	\checkmark	\checkmark	\checkmark	\checkmark	\checkmark
RBM	\checkmark	?	?	\circ	\circ	?	?	\checkmark	\checkmark	\checkmark	?	\checkmark

example, if we apply first a Hadamard gate, and then a measurement, to the state $|0\rangle|\varphi\rangle + |1\rangle|\psi\rangle$, we may obtain the state $|0\rangle \otimes (|\varphi\rangle + |\psi\rangle)$. For a data structure, this resulting state is at least as difficult to represent as the sum $|\varphi\rangle + |\psi\rangle$. Therefore, it is instructive to check which data structures support **Addition**: it allows us to explain why certain gates are not tractable for a data structure (such as the swap and general local gates). In particular, all decision diagram implementations support an explicit addition subroutine (Miller and Thornton 2006; Clarke et al. 2001). In addition, **InnerProd** and **Fidelity** (and **Local**) are required in variational methods and quantum circuit verification involves Eq.

For the operations listed above and the languages from Sec. 2, we present an overview of existing and novel tractability results in Th. 2 (Table 2). The novel results in this work are the hardness results (denoted \circ) for **InnerProd** and **Fidelity** on LIMDD and RBM (Th. 3 and for **InnerProd** we can reduce from **Fidelity**) and unsupported manipulations (denoted \times) on SLDD \times and LIMDD. More generally, our proof shows that computing **Fidelity** is hard for any data structure which succinctly represents both all graph states and the Dicke state, such as RBM and LIMDD. A fidelity algorithm for SLDD \times was mentioned by (Burgholzer, Kueng, and Wille 2021), but, to the best of our knowledge, had not previously been described or analyzed.

Theorem 2. The tractability results in Table 2 hold.

Theorem 3. Assuming the exponential time hypothesis, the fidelity of two states represented as LIMDDs or RBMs cannot be computed in polynomial time. The proof uses a reduction from the #EVEN SUBGRAPHS problem (Jerrum and Meeks 2017).

5 Rapidity of Data Structures

The tractability criterion, studied in Sec. 4, sometimes gives a skewed picture of efficiency. For example, looking naively at Table 2, it seems that ADD is faster than SLDD \times when applying a Hadamard gate. Yet there is no state for which applying the Hadamard gate on its SLDD \times representation is slower than on its ADD representation. So succinctness actually consistently mitigates the worst-case runtime behavior. To remedy this shortcoming, (Lai, Liu, and Yin 2017) introduced the notion of *rapidity* for canonical data structures.

In Def. 3, we generalize rapidity to support non-canonical data structures, such as MPS, RBM, d-DNNF (Darwiche 2001) and CCDD (Lai, Meel, and Yap 2022). To achieve this, Def. 3 requires that for a fixed input φ to ALG_1 , among all equivalent inputs to ALG_2 , there is one on which ALG_2 is at least as fast as ALG_1 . It may seem reasonable to require, instead, that ALG_2 is at least as fast as ALG_1 on all equivalent inputs; however, in general, there may be no upper bound on the size of the (infinitely many) such inputs; thus, such a requirement would always be vacuously false.

In the following, we write $time(A, x)$ for the runtime of algorithm A on input x .

Definition 3 (Rapidity for non-canonical data structures). Let D_1, D_2 be two data structures and consider some c -ary operation OP on these data structures. In the below, ALG_1 (ALG_2) is an algorithm implementing OP for D_1 (D_2).

- We say that ALG_1 is *at most as rapid as* ALG_2 if there exists a polynomial p such that for each input $\varphi = (\varphi_1, \dots, \varphi_c)$ there exists an equivalent input $\psi = (\psi_1, \dots, \psi_c)$, i.e., with $|\varphi_j\rangle = |\psi_j\rangle$ for $j = 1 \dots c$, for which $time(ALG_2, \psi) \leq p(time(ALG_1, \varphi))$. We say that ALG_2 is *at least as rapid as* ALG_1 .
- We say that $OP(D_1)$ is *at most as rapid as* $OP(D_2)$ if for each algorithm ALG_1 performing $OP(D_1)$, there is an algorithm ALG_2 performing $OP(D_2)$ such that ALG_1 is at most as rapid as ALG_2 .

We remark that, when applied to canonical data structures, Def. 3 reduces to the definition by Lai et al. , except that Lai et al. allow the input to be fully read by the algorithm: $time(ALG_1, x_1) \leq \underline{\text{poly}(time(ALG_2, x_2) + |x_2|)}$ (difference underlined). We omit this to achieve transitivity. Rapidity indeed has the desirable property that it is a preorder, i.e., it is reflexive and transitive, as Th. 4 shows.

Theorem 4. Rapidity is a preorder over data structures.

5.1 A Sufficient Condition for Rapidity

We now introduce a simple sufficient condition for rapidity in Th. 5, allowing researchers to easily establish that one data structure is more rapid than another *for many relevant operations simultaneously*. Previously, such proofs were done for each operation individually (Lai, Liu, and Yin 2017). We use this sufficient condition to establish rapidity

relations between many of the data structures studied in this work. By a *transformation* f from data structure D_1 to D_2 we mean a map such that $|f(x_1)\rangle = |x_1\rangle$ for all $x_1 \in D_1$. We also need the notions of a weakly minimizing transformation (Def. 4) and a runtime monotonic algorithm (Def. 5).

Definition 4 (Weakly minimizing transformation). Let D_1, D_2 be data structures. A transformation $f : D_1 \rightarrow D_2$ is *weakly minimizing* if f always outputs an instance which is polynomially close to minimum-size, i.e., there exists a polynomial p such that for all $x_1 \in D_1, x_2 \in D_2$ with $|x_1\rangle = |x_2\rangle$, we have $|f(x_1)| \leq p(|x_2|)$.

Definition 5 (Runtime monotonic algorithm). An algorithm ALG implementing some operation on data structure D is *runtime monotonic* if for each polynomial s there is a polynomial t such that for each state $|\varphi\rangle$ and each $x, y \in D^\varphi$, if $|x| \leq s(|y|)$, then $\text{time}(ALG, x) \leq t(\text{time}(ALG, y))$.

Theorem 5 (A sufficient condition for rapidity). Let D_1, D_2 be data structures with $D_1 \preceq_s D_2$ and OP a c -ary operation. Suppose that,

- A1 $OP(D_2)$ requires time $\Omega(m)$ where m is the sum of the sizes of the operands; and
- A2 for each algorithm ALG implementing $OP(D_2)$, there is a runtime monotonic algorithm ALG_2^{rm} , implementing the same operation $OP(D_2)$, which is at least as rapid as ALG ; and
- A3 there exists a transformation from D_1 to D_2 which is (i) weakly minimizing and (ii) runs in time polynomial in the output size (i.e, in time $\text{poly}(|\psi|)$ for transformation output $\psi \in D_2$); and
- A4 if OP is a manipulation operation (as opposed to a query), then there also exists a polynomial time transformation from D_2 to D_1 (polynomial time in the input size, i.e, in $|\rho|$ for transformation input $\rho \in D_2$).

Then D_1 is at least as rapid as D_2 for operation OP .

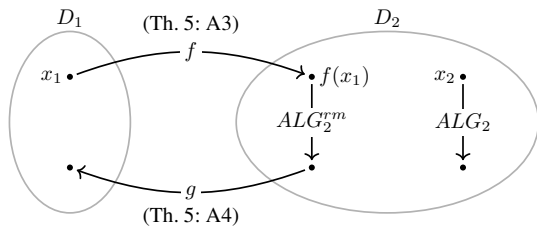


Figure 3: Visualization of the proof of Th. 5 in case OP is a transformation operation: Given runtime monotonic algorithm ALG_2^{rm} implementing OP on language D_2 , the composed algorithm $ALG_1 \triangleq g \circ ALG_2^{rm} \circ f$ for $OP(D_1)$ is at least as rapid as ALG_2 . To prove this, we consider $x_2 \in D_2$ and an equivalent and at most only polynomially larger than $x_1 \in D_1$ and show that ALG_1 takes at most polynomially more time on x_1 than ALG_2 on x_2 . ALG_1 is also runtime monotonic. Horizontally-aligned instances of data structures are equivalent, i.e. represent the same quantum state.

Fig. 3 provides a proof outline that illustrates the need for (polynomial-time) transformations in order to execute operations on states represented in data structure D_1 on their D_2 counterpart. The operation on $f(x_1)$ is at most polynomially slower than on its counterpart x_2 because f produces a small instance (because f is weakly minimizing), and because ALG_2^{rm} is not much slower on such instances (because it is runtime monotonic). We opted for weakly minimizing transformations (rather than *strictly* minimizing transformations), because a minimum structure might be hard to compute and is not needed in the proof. Runtime monotonic algorithms are ubiquitous, for instance, most operations on MPS scale polynomially in the bond dimension and number of qubits (Vidal 2003). Finally, we emphasize that for canonical data structures D , each algorithm is runtime monotonic and any transformation $D_1 \rightarrow D$ is weakly minimizing.

5.2 Rapidity between Quantum Representations

We now capitalize on the sufficient condition of Th. 5 by revealing the rapidity relations between data structures for all operations satisfying A1 and A2. Th. 6 shows our findings. We highlight the result that MPS is at least as rapid as $SLDD_\times$ in Th. 7. Its proof provides the required transformations from MPS to $SLDD_\times$ and back.

Theorem 6. The rapidity relations in Fig. 9 hold.

Theorem 7. MPS is at least as rapid as $SLDD_\times$ for all operations satisfying A1 and A2.

Proof sketch. Since $SLDD_\times$ is canonical, the runtime monotonicity (A2 of Th. 5, see Def. 5) and weakly-minimizing (A3) requirements are satisfied automatically. Hence we only need to provide efficient transformations in both directions (A3-A4): We transform $SLDD_\times$ to MPS by choosing its matrices A_k^x to be the weighted bipartite adjacency matrices of the x -edges (low / high edges) between level k and $k - 1$ nodes of the $SLDD_\times$. In the other direction, an MPS can be efficiently transformed into an $SLDD_\times$ by contracting the first open index with $|0\rangle$ and then $|1\rangle$ to find the coefficients in the $|0\rangle$ and $|1\rangle$ parts of the state's Shannon decomposition; and repeating this recursively for all possible partial assignments. Dynamic programming using the fidelity operation (efficient for MPS) ensures that only a polynomial number of recursive calls are made. \square

The relations not involving MPS involve QDDs. QDDs are canonical data structures as explained in Sec. 2, so that runtime monotonicity and weak minimization of transformations are automatically ensured. Transformations between different QDDs can be realized using the well-known MAKENODE procedure (see Sec. 2), in linear time in the resulting QDD size (using dynamic programming).

6 Related work

(Darwiche and Marquis 2002) pioneered the knowledge compilation map approach followed here. (Fargier et al.

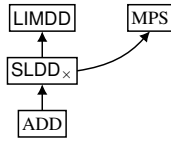


Figure 4: Rapidity relations between data structures considered here. A solid arrow $D_1 \rightarrow D_2$ means D_2 is at least as rapid as D_1 for all operations satisfying A1 and A2 of Th. 5.

2014) employ the same method to compare decision diagrams for real-valued functions. In order to mend a deficiency in the notion of tractability, (Lai, Liu, and Yin 2017) contributed the notion of *rapidity*, which we extend in Sec. 5

Alternative ways to deal with non-canonical data structures includes finding a canonical variant, as has been done for MPS (Perez-Garcia et al. 2007), although it is not canonical for all states. For other structures, such as RBM, d-DNNF and CCDD (mentioned before) such canonical versions do not exist as far as we know, and might not be tractable.

Often the differences between DD variants in Table 1 are subtle differences in the constraints used for obtaining canonicity. While perhaps irrelevant for the (asymptotic) analysis, we emphasize that these definitions have great practical relevance. For instance, canonicity makes dynamic programming efficient, which enables fast implementations of QDD operations, while it also reduces the diagram size. Moreover, in practice the behavior of floating point calculations interacts with the canonicity constraints (Zulehner, Hillmich, and Wille 2019), significantly affecting performance. Like (Fargier et al. 2014), we do not analyze numerical stability and focus on asymptotic behavior.

The affine algebraic decision diagram (AADD), introduced by (Sanner and McAllester 2005), augments the SLDD_\times as shown in Table 1. Their work proves that the worst-case time and space performance of AADD is within a multiplicative factor of that of ADD. The concept of rapidity makes explicit that this is the case only when equivalent inputs are considered for both structures. We note that AADD would be able to represent $|\text{Sum}\rangle$ (a hard case for all QDDs studied here), so its succinctness relation with respect to RBM is still open. We omit Affine ADD (AADD) (Sanner and McAllester 2005), since to the best of our knowledge these have not been applied to quantum computing yet. The LIMDD data structure is implemented and compared against SLDD_\times in (Vinkhuijzen et al. 2023b).

(Burgholzer, Ploier, and Wille 2023) compare tensor networks, including MPS, to decision diagrams, on slightly different criteria, such as abstraction level and ease of distributing the computational workload on a supercomputer. Hong et al. introduce the Tensor Decision Diagram, which extends the SLDD_\times so that it is able to represent tensors (Hong et al. 2022) and their contraction. Context-Free-Language Ordered Binary Decision Diagrams (CFLOBDDs) (Sistla, Chaudhuri, and Reps 2023a,c,b) achieve a similar goal by extending BDDs with insights from visibly pushdown au-

tomata (Alur and Madhusudan 2004).

The stabilizer formalism is a tractable but non-universal method to represent and manipulate quantum states (Aaronson and Gottesman 2004). Its universal counterpart is the stabilizer decomposition-based method (Bravyi, Smith, and Smolin 2016), which relies on a linear combination of representations in the stabilizer formalism that is exponential only in the number of T gates in the circuit. Although this is a highly versatile technique (Bravyi and Gosset 2016), no superpolynomial lower bounds on their size are known at the moment, making it less useful to include them in a knowledge compilation map.

Similarly, we expect the relation between tree tensor networks (Orús 2014) and SDDs (Darwiche 2011) to be similar the relation between SLDD_\times and MPS, since SDD also extend the linear QDD variable order with a ‘variable tree.’

(Ablayev, Gainutdinova, and Karpinski 2001) introduce the Quantum Branching Program, a branching program whose state is a superposition of the nodes on a given level, some of which are labeled *accepting*. An input string $x \in \{0, 1\}^n$ determines how the superposition evolves. A string $x \in \{0, 1\}^n$ is said to be accepted by the automaton if, after evolving according to x , a measurement causes the superposition to collapse to an accepting state with probability greater than $\frac{1}{2}$. Thus, the automaton accepts a finite language $L \subseteq \{0, 1\}^n$. Since this diagram accepts a language, rather than represents and manipulates a quantum state, we cannot properly fit it into the present knowledge compilation map.

7 Discussion

We have compared several classical data structures for representing quantum information on their succinctness, tractability of relevant operations and rapidity. We catalogued all relevant operations required to implement simulation of quantum circuits, variational quantum algorithms (e.g., quantum machine learning) and quantum circuit verification. We have followed the approach of (Darwiche and Marquis 2002) and (Fargier et al. 2014) to map the succinctness and tractability of the data structures. In order to mend a deficiency in the notion of tractability that was noticed by several researchers, we additionally adopt and develop the framework of *rapidity*. We contribute a general-purpose method by which data structures, whether canonical or not, may be analytically compared on their rapidity.

Common knowledge says that there is a trade-off between the succinctness, and the speed of a data structure. In contrast, we find that, the more succinct data structures are often also more rapid. For example, we find that algebraic decision diagrams, SLDD_\times , and matrix product states are each successively more succinct and more rapid. However, in practice, the SLDD_\times has achieved striking performance on realistic benchmarks, (Zulehner and Wille 2018) due to a successful sustained effort to optimize the software implementation. But we emphasize that e.g. MPS was not developed with the intention for circuit simulation but for quantum sim-

ulation, and $SLDD_{\times}$ is vice versa. Therefore, more research is needed to compare the relative performance of these data structures on the various application domains in practice.

In future work, we could also consider unbounded operations (multiple applications of the same gates) and other data structures, e.g., tree tensor networks (Orús 2014) and affine algebraic decision diagrams (Sanner and McAllester 2005).

References

- Aaronson, S.; and Gottesman, D. 2004. Improved simulation of stabilizer circuits. *Physical Review A*, 70(5).
- Ablyayev, F.; Gainutdinova, A.; and Karpinski, M. 2001. On computational power of quantum branching programs. In *Fundamentals of Computation Theory: 13th International Symposium, FCT 2001 Riga, Latvia, August 22–24, 2001 Proceedings 13*, 59–70. Springer.
- Alur, R.; and Madhusudan, P. 2004. Visibly Pushdown Languages. In *Proceedings of the Thirty-Sixth Annual ACM Symposium on Theory of Computing*, STOC '04, 202–211. New York, NY, USA: Association for Computing Machinery. ISBN 1581138520.
- Ardeshir-Larijani, E.; Gay, S. J.; and Nagarajan, R. 2014. Verification of Concurrent Quantum Protocols by Equivalence Checking. In *TACAS*, 500–514. Springer.
- Audemard, G.; Koriche, F.; and Marquis, P. 2020. On tractable XAI queries based on compiled representations. In *Proceedings of the International Conference on Principles of Knowledge Representation and Reasoning*, volume 17, 838–849.
- Bahar, R. I.; Frohm, E. A.; Gaona, C. M.; Hachtel, G. D.; Macii, E.; Pardo, A.; and Somenzi, F. 1997. Algebraic decision diagrams and their applications. *Formal methods in system design*, 10(2-3): 171–206.
- Bärtschi, A.; and Eidenbenz, S. 2019. Deterministic preparation of Dicke states. In *Fundamentals of Computation Theory: 22nd International Symposium, FCT 2019, Copenhagen, Denmark, August 12–14, 2019, Proceedings 22*, 126–139. Springer.
- Benedetti, M.; Lloyd, E.; Sack, S.; and Fiorentini, M. 2019. Parameterized quantum circuits as machine learning models. *Quantum Science and Technology*, 4(4): 043001.
- Blanca, A.; Chen, Z.; Štefankovič, D.; and Vigoda, E. 2021. Hardness of identity testing for restricted Boltzmann machines and Potts models. *The Journal of Machine Learning Research*, 22(1): 6727–6782.
- Bollig, B.; and Wegener, I. 1996. Improving the variable ordering of OBDDs is NP-complete. *IEEE Transactions on Computers*, 45: 993–1002.
- Bova, S. 2016. SDDs are exponentially more succinct than OBDDs. In *Thirtieth AAAI Conference on Artificial Intelligence*.
- Brace, K. S.; Rudell, R. L.; and Bryant, R. E. 1990. Efficient implementation of a BDD package. In *27th ACM/IEEE design automation conference*, 40–45. IEEE.
- Bravyi, S.; and Gosset, D. 2016. Improved Classical Simulation of Quantum Circuits Dominated by Clifford Gates. *Phys. Rev. Lett.*, 116: 250501.
- Bravyi, S.; and Kitaev, A. 2005. Universal quantum computation with ideal Clifford gates and noisy ancillas. *Phys. Rev. A*, 71: 022316.
- Bravyi, S.; Smith, G.; and Smolin, J. A. 2016. Trading Classical and Quantum Computational Resources. *Phys. Rev. X*, 6: 021043.
- Bryant, R. E. 1986. Graph-Based Algorithms for Boolean Function Manipulation. *IEEE Trans. Computers*, 35(8): 677–691.
- Burgholzer, L.; Kueng, R.; and Wille, R. 2021. Random stimuli generation for the verification of quantum circuits. In *Proceedings of the 26th Asia and South Pacific Design Automation Conference*, 767–772.
- Burgholzer, L.; Ploier, A.; and Wille, R. 2023. Tensor Networks or Decision Diagrams? Guidelines for Classical Quantum Circuit Simulation. *arXiv preprint arXiv:2302.06616*.
- Burgholzer, L.; and Wille, R. 2020. Advanced equivalence checking for quantum circuits. *IEEE Transactions on Computer-Aided Design of Integrated Circuits and Systems*, 40(9): 1810–1824.
- Carleo, G.; and Troyer, M. 2017. Solving the quantum many-body problem with artificial neural networks. *Science*, 355(6325): 602–606.
- Chen, J.; Cheng, S.; Xie, H.; Wang, L.; and Xiang, T. 2018. Equivalence of restricted Boltzmann machines and tensor network states. *Physical Review B*, 97(8): 085104.
- Clarke, E. M.; Fujita, M.; McGeer, P. C.; McMillan, K.; Yang, J. C.-Y.; and Zhao, X. 2001. Multi-Terminal Binary Decision Diagrams: An Efficient Data Structure for Matrix Representation.
- Clarke, E. M.; McMillan, K. L.; Zhao, X.; Fujita, M.; and Yang, J. 1993. Spectral transforms for large boolean functions with applications to technology mapping. In *Proceedings of the 30th international Design Automation Conference*, 54–60.
- Dang, A.; Hill, C. D.; and Hollenberg, L. C. L. 2019. Optimising Matrix Product State Simulations of Shor’s Algorithm. *Quantum*, 3: 116.
- Darwiche, A. 2001. Decomposable negation normal form. *Journal of the ACM (JACM)*, 48(4): 608–647.
- Darwiche, A. 2011. SDD: a new canonical representation of propositional knowledge bases. In *Proceedings of the Twenty-Second international joint conference on Artificial Intelligence-Volume Volume Two*, 819–826. AAAI Press.
- Darwiche, A.; and Marquis, P. 2002. A knowledge compilation map. *Journal of Artificial Intelligence Research*, 17: 229–264.
- Dicke, R. H. 1954. Coherence in spontaneous radiation processes. *Physical review*, 93(1): 99.
- Dumoulin, V.; Goodfellow, I.; Courville, A.; and Bengio, Y. 2014. On the Challenges of Physical Implementations of

- RBM. *Proceedings of the AAAI Conference on Artificial Intelligence*, 28(1).
- Dunjko, V.; and Briegel, H. J. 2017. Machine learning & artificial intelligence in the quantum domain. arXiv:1709.02779.
- Fargier, H.; Marquis, P.; Niveau, A.; and Schmidt, N. 2014. A knowledge compilation map for ordered real-valued decision diagrams. In *Proceedings of the AAAI Conference on Artificial Intelligence*, volume 28.
- Fargier, H.; Marquis, P.; and Schmidt, N. 2013. Semiring Labelled Decision Diagrams, Revisited: Canonicity and Spatial Efficiency Issues. In *IJCAI*, 884–890.
- Foulkes, W.; Mitas, L.; Needs, R.; and Rajagopal, G. 2001. Quantum Monte Carlo simulations of solids. *Reviews of Modern Physics*, 73(1): 33.
- Gay, S. J.; and Nagarajan, R. 2005. Communicating quantum processes. In *Proceedings of the 32nd ACM SIGPLAN-SIGACT Symposium on Principles of Programming Languages*, 145–157.
- Glasser, I.; Sweke, R.; Pancotti, N.; Eisert, J.; and Cirac, I. 2019. Expressive power of tensor-network factorizations for probabilistic modeling. *Advances in neural information processing systems*, 32.
- Hong, X.; Zhou, X.; Li, S.; Feng, Y.; and Ying, M. 2022. A Tensor Network Based Decision Diagram for Representation of Quantum Circuits. *ACM Trans. Des. Autom. Electron. Syst.*, 27(6).
- Jerrum, M.; and Meeks, K. 2017. The parameterised complexity of counting even and odd induced subgraphs. *Combinatorica*, 37(5): 965–990.
- Jones, T.; Brown, A.; Bush, I.; and Benjamin, S. C. 2019. QuEST and high performance simulation of quantum computers. *Scientific reports*, 9(1): 1–11.
- Jónsson, B.; Bauer, B.; and Carleo, G. 2018. Neural-network states for the classical simulation of quantum computing. *arXiv preprint arXiv:1808.05232*.
- Knuth, D. E. 2005. *The Art of Computer Programming. Volume 4, Fascicle 1*. Addison-Wesley.
- Lai, Y.; Liu, D.; and Yin, M. 2017. New canonical representations by augmenting OBDDs with conjunctive decomposition. *Journal of Artificial Intelligence Research*, 58: 453–521.
- Lai, Y.; Meel, K. S.; and Yap, R. H. 2022. CCDD: A Tractable Representation for Model Counting and Uniform Sampling. *arXiv preprint arXiv:2202.10025*.
- Lai, Y.-T.; Pedram, M.; and Vrudhula, S. B. 1994. EVBDD-based algorithms for integer linear programming, spectral transformation, and function decomposition. *IEEE Transactions on Computer-Aided Design of Integrated Circuits and Systems*, 13(8): 959–975.
- Martens, J.; Chattopadhyaya, A.; Pitassi, T.; and Zemel, R. 2013. On the representational efficiency of restricted Boltzmann machines. *Advances in Neural Information Processing Systems*, 26.
- Miller, D. M.; and Thornton, M. A. 2006. QMDD: A decision diagram structure for reversible and quantum circuits. In *36th International Symposium on Multiple-Valued Logic (ISMVL'06)*, 30–30. IEEE.
- Nielsen, M. A.; and Chuang, I. L. 2000. Quantum information and quantum computation. *Cambridge: Cambridge University Press*, 2(8): 23.
- Orús, R. 2014. A practical introduction to tensor networks: Matrix product states and projected entangled pair states. *Annals of Physics*, 349: 117–158.
- Perez-Garcia, D.; Verstraete, F.; Wolf, M.; and Cirac, J. 2007. Matrix product state representations. *Quantum Information & Computation*, 7(5): 401–430.
- Sanner, S.; and McAllester, D. 2005. Affine Algebraic Decision Diagrams (AADDs) and Their Application to Structured Probabilistic Inference. In *Proceedings of the 19th International Joint Conference on Artificial Intelligence, IJCAI'05*, 1384–1390. San Francisco, CA, USA: Morgan Kaufmann Publishers Inc.
- Schollwöck, U. 2011. The density-matrix renormalization group in the age of matrix product states. *Annals of physics*, 326(1): 96–192.
- Sistla, M.; Chaudhuri, S.; and Reps, T. 2023a. CFLOB-DDs: Context-Free-Language Ordered Binary Decision Diagrams. arXiv:2211.06818.
- Sistla, M.; Chaudhuri, S.; and Reps, T. 2023b. Symbolic Quantum Simulation with Quasimodo. In Enea, C.; and Lal, A., eds., *Computer Aided Verification*, 213–225. Cham: Springer Nature Switzerland. ISBN 978-3-031-37709-9.
- Sistla, M.; Chaudhuri, S.; and Reps, T. 2023c. Weighted Context-Free-Language Ordered Binary Decision Diagrams. arXiv:2305.13610.
- Somenzi, F. 1999. Binary decision diagrams. In Broy, M.; and Steinbrüggen, R., eds., *Computational system design*, 303–366. IOS.
- Tafertshofer, P.; and Pedram, M. 1997. Factored edge-valued binary decision diagrams. *Formal Methods in System Design*, 10(2): 243–270.
- Thanos, D.; Coopmans, T.; Laarman, A.; and . 2023. Fast equivalence checking of quantum circuits of Clifford gates. arXiv:2308.01206.
- Torlai, G.; Mazzola, G.; Carrasquilla, J.; Troyer, M.; Melko, R.; and Carleo, G. 2018. Neural-network quantum state tomography. *Nature Physics*, 14(5): 447–450.
- Van den Nest, M.; Dehaene, J.; and De Moor, B. 2004. Graphical description of the action of local Clifford transformations on graph states. *Physical Review A*, 69(2): 022316.
- Vandaele, V.; Martiel, S.; Perdrix, S.; and Vuillot, C. 2023. Optimal Hadamard gate count for Clifford +T synthesis of Pauli rotations sequences. *arXiv preprint arXiv:2302.07040*.
- Viamontes, G. F.; Markov, I. L.; and Hayes, J. P. 2003. Improving gate-level simulation of quantum circuits. *Quantum Information Processing*, 2(5): 347–380.
- Vidal, G. 2003. Efficient classical simulation of slightly entangled quantum computations. *Physical review letters*, 91(14): 147902.

Vinkhuijzen, L.; Coopmans, T.; Elkouss, D.; Dunjko, V.; and Laarman, A. 2023a. LIMDD: a decision diagram for simulation of quantum computing including stabilizer states. *Quantum*, 7.

Vinkhuijzen, L.; Grurl, T.; Hillmich, S.; Brand, S.; Wille, R.; and Laarman, A. 2023b. Efficient Implementation of LIMDDs for Quantum Circuit Simulation. In Caltais, G.; and Schilling, C., eds., *Model Checking Software*, 3–21. Springer. ISBN 978-3-031-32157-3.

Wegener, I. 2000. *Branching programs and binary decision diagrams: theory and applications*. SIAM.

Wilson, N. 2005. Decision diagrams for the computation of semiring valuations. In *Proceedings of the 19th international joint conference on Artificial intelligence*, 331–336.

Wu, Y.; Duan, L.-M.; and Deng, D.-L. 2020. Artificial neural network based computation for out-of-time-ordered correlators. *Phys. Rev. B*, 101: 214308.

Zhang, Y.-H.; Jia, Z.; Wu, Y.-C.; and Guo, G.-C. 2018. An efficient algorithmic way to construct Boltzmann machine representations for arbitrary stabilizer code. *arXiv:1809.08631*.

Zulehner, A.; Hillmich, S.; and Wille, R. 2019. How to efficiently handle complex values? Implementing decision diagrams for quantum computing. In *2019 IEEE/ACM International Conference on Computer-Aided Design (ICCAD)*, 1–7. IEEE.

Zulehner, A.; and Wille, R. 2018. Advanced simulation of quantum computations. *IEEE Transactions on Computer-Aided Design of Integrated Circuits and Systems*, 38(5): 848–859.

A Additional Preliminaries on Quantum Information and Decision Diagrams

A.1 Brief Introduction to Quantum Information

This appendix presents additional background on quantum information necessary to understand the other appendices. For a detailed treatment, we refer to (Nielsen and Chuang 2000).

The basic unit of quantum information is a quantum bit or *qubit*. The joint state φ of n qubits is described by a unit vector of 2^n complex numbers, denoted $|\varphi\rangle$ in Dirac notation. Equivalently, a state φ is described by an *amplitude function* $f_\varphi: \{0, 1\}^n \rightarrow \mathbb{C}$ satisfying $\sum_{\vec{x} \in \{0, 1\}^n} |f_\varphi(\vec{x})|^2 = 1$. Here a complex number $z = a + bi$ with $a, b \in \mathbb{R}$ has squared modulus $|z|^2 = z^* \cdot z = a^2 + b^2$ and complex conjugate $z^* = a - bi$. The computational basis of the n -qubit vector space \mathbb{C}^{2^n} is $|k\rangle = (0, 0, \dots, 0, 1, 0, \dots, 0)^T$ for $k \in \{0, 1, \dots, 2^n - 1\}$, where the single entry 1 occurs at the k -th position (often we write k in binary, i.e. $k \in \{0, 1\}^n$) and $(\cdot)^T$ denotes vector transposition. Thus $|\varphi\rangle = \sum_{x \in \{0, 1\}^n} f_\varphi(x) |x\rangle$. We also write $|k\rangle = |x_1 x_2 \dots x_n\rangle = |x_1\rangle \otimes |x_2\rangle \otimes \dots \otimes |x_n\rangle$ for $x_j \in \{0, 1\}$ and x the binary representation of $k \in \mathbb{N}_{\geq 0}$. Here $A \otimes B$ for a $k \times l$ matrix A and an $m \times n$ matrix B is the $km \times ln$ tensor product:

$$A \otimes B = \begin{pmatrix} A_{00}B & A_{01}B & \dots & A_{0l}B \\ A_{10}B & A_{11}B & \dots & A_{1l}B \\ \vdots & \vdots & \ddots & \vdots \\ A_{k0}B & A_{k1}B & \dots & A_{kl}B \end{pmatrix}.$$

Two separate quantum states $|\varphi_A\rangle, |\varphi_B\rangle$ on n_A, n_B qubits have joint state $|\varphi_A\rangle \otimes |\varphi_B\rangle$. If a quantum state $|\varphi\rangle$ on $n = n_A + n_B$ qubits is decomposable as $|\varphi\rangle = |\varphi_A\rangle \otimes |\varphi_B\rangle$, it is *separable* (with respect to bipartition A, B) and *entangled* otherwise. We say that a complex vector $|\varphi\rangle \in \mathbb{C}^{2^n}$ is *normalized* when $|\varphi\rangle$ is a unit vector.

Two quantum states φ, ψ are *equivalent* iff there exists a complex value $\lambda \in \mathbb{C}$ such that $|\varphi\rangle = \lambda \cdot |\psi\rangle$. Given two n -qubit states φ, ψ , their inner product is $\langle \varphi | \psi \rangle \triangleq \sum_{\vec{x} \in \{0, 1\}^n} f_\varphi(\vec{x})^* \cdot f_\psi(\vec{x})$, and their fidelity is $|\langle \varphi | \psi \rangle|^2$. Equivalently, the inner product is also (the 1×1 -matrix entry) $\langle \varphi | \cdot | \varphi \rangle$ where $\langle \varphi | \triangleq (|\varphi\rangle)^\dagger$ is a column vector where $(\cdot)^\dagger$ is the complex transpose operator, which first takes a matrix's transpose followed by entry-wise complex conjugation. Note that if $k \in \{0, 1\}^n$, the k -th entry in the state vector $|\varphi\rangle$ is $\langle k | \varphi \rangle = f_\varphi(k)$.

Example 1. Fig. 1 gives an example of a quantum state on 3 qubits, the so-called GHZ state: $|\text{GHZ}\rangle = 1/\sqrt{2}(|000\rangle + |111\rangle)$. This state is displayed as state vector (left), followed by representations in all data structures used in this paper.

A quantum state can be manipulated by applying a quantum *gate* or a measurement to it. An n -qubit gate U is a unitary transformation $U: \mathbb{C}^{2^n} \rightarrow \mathbb{C}^{2^n}$, i.e., it satisfies $U^\dagger U = U U^\dagger = \mathbb{I}_{2^n}$ where \mathbb{I}_{2^n} is the n -qubit identity operator mapping each vector to itself. Examples of gates are the four Pauli matrices defined in Sec. 2.2, the controlled- U gate mapping $|0\rangle \otimes |\varphi\rangle$ to itself and $|1\rangle \otimes |\varphi\rangle$ to $|1\rangle \otimes U|\varphi\rangle$, the Hadamard gate $H = 1/\sqrt{2} \begin{bmatrix} 1 & 1 \\ 1 & -1 \end{bmatrix}$, the gate $T = \begin{bmatrix} 1 & 0 \\ 0 & e^{i/4\pi} \end{bmatrix}$ and the phase gate $S = T^2$. A single-qubit computational-basis measurement, performed on the k -th qubit of an n -qubit state φ , yields outcome $m \in \{0, 1\}$ with probability $p_m \triangleq \sum_{x \in \{0, 1\}^{n-1}} |f_\varphi(x, x_k = m)|^2$, and the post-measurement state ψ is found by setting a vector entries with $x_k \neq m$ to 0 and subsequent rescaling; i.e., $f_\psi(x) := f_\varphi(x)/p_m$ if $x_k = m$ and $f_\psi(x) := 0$ otherwise.

Example 2. A small quantum circuit is shown in Fig. 5. The initial state is $|0\rangle \otimes |0\rangle \otimes |0\rangle$. First, a Hadamard gate is applied to the first qubit, after which the state becomes $1/\sqrt{2}(|000\rangle + |100\rangle)$. Then a controlled- X gate is applied to the first and second qubit. Here the first qubit acts as the control; the second qubit is the target. The state of the quantum system is now $1/\sqrt{2}(|000\rangle + |110\rangle)$. The state before measurement is called the GHZ state, $|\text{GHZ}\rangle = 1/\sqrt{2}(|000\rangle + |111\rangle)$. Finally, a measurement is applied to the third qubit. After this measurement, the state “collapses” to either state $|000\rangle$ or $|111\rangle$ with equal probability.

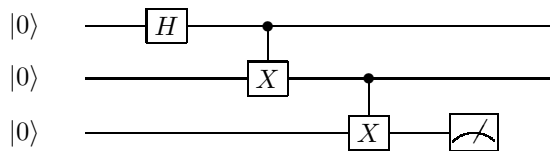


Figure 5: 3-qubit quantum circuit preparing the GHZ state.

We now formalize the application domains from Sec. 1. In *circuit simulation*, a quantum circuit consists of (i) an initial quantum

state, (ii) several quantum gates followed by (iii) measuring one or more quantum bits.[†] Simulating a circuit using the data structures in this work starts by constructing a data structure for (i), followed by manipulating the data structure by applying the gates and measurements of (ii) one by one. The structure supports *strong simulation* if it can produce the probability function; or *weak simulation* if it merely produces a sample, for each measurement in (iii). Next, the quantum circuit of *variational methods* consist of a quantum circuit; then the output state $|\varphi\rangle$ is used to compute $\langle\varphi|O|\varphi\rangle$ for some linear operator O (an *observable*) which is hermitian ($O = O^\dagger$), for example O is the Hamiltonian. This computation reduces to $\langle\varphi|\psi\rangle$ with $|\psi\rangle := O|\varphi\rangle$ which could be any complex vector. Often one considers *local* observables. Specifically, an n -qubit observable O is called k -local when it can be written as $O = P \otimes \mathbb{I}_{2^{n-k}}$ where P is a k -qubit observable. Last, *circuit verification* relies on checking approximate or exact equivalence of quantum states. This extends to unitaries, which all data structures from this paper can represent also, but which we will not treat for simplicity.

A.2 Preliminaries on decision diagrams

Here, we present some additional background required to understand the results in the other appendices. For a detailed treatment of decision diagrams, we refer to (Somenzi 1999).

The tractability of the QDD algorithms heavily relies on two properties: canonicity, i.e., there exists a unique decision diagram for each quantum state, and dynamic programming, i.e., avoiding unnecessary recursion by storing intermediary results in a cache. Canonicity implies that for each quantum state φ there is a unique diagram $x \in D^\varphi$, and moreover no other (non-canonical) data structure $y \in D^\varphi$ has fewer nodes or edges than x . All QDDs in this work can be made canonical by requiring that the QDD satisfies a set of reduction rules (for SLDD $_\times$ see (Miller and Thornton 2006) and for LIMDD see (Vinkhuijzen et al. 2023a)) and all isomorphic nodes are subsequently merged (see Table 1). This so-called *reduced* QDD can be obtained in linear time using a standard MAKENODE procedure (see also Sec. 5.2). QDD manipulation algorithms also use the MAKENODE procedure to ensure that the result is reduced efficiently. For these reasons, we may always assume that QDDs are reduced.

Let $f: \{0, 1\}^n \rightarrow \mathbb{C}$ be a function, and $y_n, y_{n-1}, \dots, y_k \in \{0, 1\}$ a partial assignment. Then $f_y: \{0, 1\}^{k-1} \rightarrow \mathbb{C}$ is the *subfunction of f induced by y* , defined as $f_y(x) = f(y, x)$. Suppose a QDD has root node v representing a pseudo-Boolean function $f: \{0, 1\}^n \rightarrow \mathbb{C}$. For any y_n, \dots, y_k , this diagram contains a node w which represents the induced subfunction $f_y: \{0, 1\}^{k-1} \rightarrow \mathbb{C}$, or which represents a function which is isomorphic to f_y under \mathcal{E}_k . The vertices of the QDD are divided into *layers*, i.e., a node which is k edges away from a leaf is said to be in layer k , and each edge points from a vertex in layer k to a node in layer $k - 1$. Each node in layer k represents a pseudo-Boolean function of the form $f: \{0, 1\}^k \rightarrow \mathbb{C}$.

We will use the following proposition as a general intuition in many of the following proofs.

Proposition 1. A reduced QDD representing pseudo-Boolean function (quantum state) f has as many nodes on level ℓ , as there are unique induced subfunctions $f_{\vec{a}}$ for $\vec{a} \in \{0, 1\}^{n-\ell}$, modulo isomorphism under \mathcal{E}_k (see Def. 2).

B Proofs of Sec. 3

In this appendix, we prove Th. 1 as reproduced below. We also reproduce Fig. 2 in Fig. 6, which additionally includes references to the respective lemmas. App. A contains relevant preliminaries on quantum information and QDDs.

Theorem 1. The succinctness results in Fig. 2 hold.

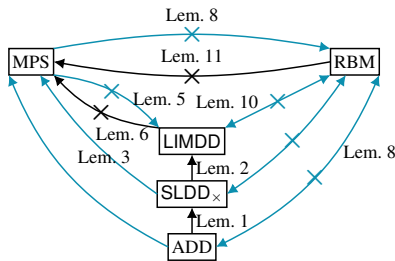


Figure 6: Succinctness relations between various classical data structures for representing quantum states. Solid arrows $A \rightarrow B$ denote $B \prec_s A$, i.e., B is strictly more succinct than A . Crossed arrows $A \not\rightarrow B$ denote a separation $B \not\prec_s A$; a bidirectional crossed arrow implies incomparability. Blue arrows indicate novel relations that we identified.

[†]In general, these steps can be intertwined and include adaptive operations, i.e. which depend on measurement outcomes, with (i) replaced by resetting the quantum state.

Proof. The proofs for individual relations are stated in the lemmas referenced by Fig. 6, which is otherwise equal to Fig. 2.

Note that we do not include a proof for every arrow (direction), since several can be derived through transitivity properties. All unlabeled edge (directions) can be derived as follows:

- $\text{MPS} \prec_s \text{ADD}$ follows from $\text{MPS} \prec_s \text{SLDD}_\times$ and $\text{SLDD}_\times \prec_s \text{ADD}$
- $\text{LIMDD} \prec_s \text{ADD}$ follows from $\text{LIMDD} \prec_s \text{SLDD}_\times$ and $\text{SLDD}_\times \prec_s \text{ADD}$
- $\text{SLDD}_\times \not\prec_s \text{RBM}$ follows from $\text{LIMDD} \not\prec_s \text{RBM}$ and $\text{LIMDD} \prec_s \text{SLDD}_\times$
- $\text{ADD} \not\prec_s \text{RBM}$ follows from $\text{LIMDD} \not\prec_s \text{RBM}$ and $\text{LIMDD} \prec_s \text{ADD}$
- $\text{RBM} \not\prec_s \text{MPS}$ follows from $\text{RBM} \not\prec_s \text{ADD}$ and $\text{MPS} \prec_s \text{ADD}$
- $\text{RBM} \not\prec_s \text{SLDD}_\times$ follows from $\text{RBM} \not\prec_s \text{ADD}$ and $\text{SLDD}_\times \prec_s \text{ADD}$
- $\text{RBM} \not\prec_s \text{LIMDD}$ follows from $\text{RBM} \not\prec_s \text{ADD}$ and $\text{LIMDD} \prec_s \text{ADD}$

This completes the proof of all stated succinctness relations. \square

Lemma 1. SLDD_\times is exponentially more succinct than ADD .

Proof. Since ADD is a special case of SLDD_\times (Sec. 2.2), SLDD_\times is at least as succinct.

(Fargier, Marquis, and Schmidt 2013) prove an exponential separation in Prop. 10. The proposition itself only mentions a superpolynomial separation; the fact that the separation is in fact exponential is contained in the proof. \square

Lemma 2. LIMDD is exponentially more succinct than SLDD_\times .

Proof. Since SLDD_\times is a special case of LIMDD (Sec. 2.2), LIMDD is at least as succinct.

(Vinkhuijzen et al. 2023a) show an exponential separation for so-called ‘cluster states.’ \square

Lemma 3. MPS is exponentially more succinct than SLDD_\times .

Proof. We show in App. D.4 that MPS is at least as succinct as SLDD_\times , by showing that every SLDD_\times can be translated to MPS in linear time.

We provide a state $|\varphi\rangle$ on n qubits, which has an exponential-sized SLDD_\times , but a polynomial-sized MPS . Let $(x)_2 \in \mathbb{Z}$ be the integer represented by a bit-string $x \in \{0, 1\}^n$. The state of interest is

$$|\varphi\rangle = \sum_{x \in \{0,1\}^n} (x)_2 |x\rangle = \sum_{x \in \{0,1\}^n} \left(\sum_{j=1}^n 2^{j-1} x_j \right) |x\rangle \quad (2)$$

(Fargier, Marquis, and Schmidt 2013) show that this state has exponential-sized SLDD_\times (Prop. 10). On the other hand, it can be efficiently represented by the following MPS of bond dimension 2:

$$A_n^0 = [1 \ 0] \quad A_j^0 = \begin{bmatrix} 1 & 0 \\ 0 & 1 \end{bmatrix} \quad A_1^0 = \begin{bmatrix} 0 \\ 1 \end{bmatrix} \quad (3)$$

$$A_n^1 = [1 \ 2^{n-1}] \quad A_j^1 = \begin{bmatrix} 1 & 2^{j-1} \\ 0 & 1 \end{bmatrix} \quad A_1^1 = \begin{bmatrix} 1 \\ 1 \end{bmatrix} \quad (4)$$

Here j ranges from $2 \dots n - 1$. To show this, we can write

$$A_n^{x_n} \dots A_1^{x_1} = [1 \ x_n \cdot 2^{n-1}] \quad A_j^{x_j} = \begin{bmatrix} 1 & x_j \cdot 2^{j-1} \\ 0 & 1 \end{bmatrix} \quad \text{for } j = 2, \dots, n - 1 \quad A_1^{x_1} = \begin{bmatrix} x_1 \\ 1 \end{bmatrix}$$

Hence we can write

$$A_n^{x_n} \dots A_1^{x_1} = [1 \ x_n \cdot 2^{n-1}] \cdot \begin{bmatrix} 1 & \sum_{j=2}^{n-1} x_j \cdot 2^{j-1} \\ 0 & 1 \end{bmatrix} \cdot \begin{bmatrix} x_1 \\ 1 \end{bmatrix} = [1 \ x_n \cdot 2^{n-1}] \cdot \begin{bmatrix} \sum_{j=1}^{n-1} x_j \cdot 2^{j-1} \\ 1 \end{bmatrix} = [\sum_{j=1}^n 2^{j-1} \cdot x_j]$$

\square

The following quantum state, called $|\text{Sum}\rangle$, will feature in several of the below proofs. Specifically, we will show that RBM and MPS can represent this state efficiently, whereas LIMDDs cannot. A similar state will be used to show that LIMDD does not support the Swap operation. We omit normalization factors, as all data structures are oblivious to them.

$$|\text{Sum}\rangle = |+\rangle^{\otimes n} + \bigotimes_{j=1}^n (|0\rangle + e^{i\pi 2^{-j-1}} |1\rangle) \quad (5)$$

Lemma 4. The LIMDD of $|\text{Sum}\rangle$ has size $2^{\Omega(n)}$ for every variable order.

Proof. We compute that the amplitude function for $|\text{Sum}\rangle$ is

$$f(\vec{x}) = 1 + e^{i\pi \sum_{j=1}^n x_j \cdot 2^{-j-1}}. \quad (6)$$

We note that f is injective and never zero, and that $\frac{f(\vec{x})}{f(\vec{y})}$ is injective on the domain where $\vec{x} \neq \vec{y}$.

We now study the nodes v at level 1 (with $\text{id}_X(v) = 1$) via the subfunctions they represent, considering all variable orders. These nodes represent subfunctions on one variable. So we take out one variable $x_k \in \vec{x} = \{x_1, \dots, x_n\}$. Without loss of generality, we may pick x_1 because the summation in Eq. (6) is commutative. For each assignment $\vec{a} \in \{0, 1\}^{n-1}$, we obtain the function:

$$f_{\vec{a}}(x_1) = 1 + e^{i\pi \sum_{j=2}^n a_j \cdot 2^{-j-1}} \cdot e^{i\pi \cdot 1/4x_1}.$$

We now show that for any $\vec{a} \neq \vec{c} \in \{0, 1\}^{n-1}$ there is no $Q \in \text{PAULILIM}_1$ such that $f_{\vec{a}} = Qf_{\vec{c}}$.

Let $Q = \alpha P$ for $\alpha \in \mathbb{C} \setminus \{0\}$, $P \in \{\mathbb{I}, X, Y, Z\}$, so $f_{\vec{a}} = \alpha P f_{\vec{c}}$. Furthermore, define $\alpha = \alpha(z, x, \vec{a}, x_1) = (-1)^z \cdot \frac{f_{\vec{a}}(x_1 \oplus x=0)}{f_{\vec{a}}(x_1 \oplus x=1)}$ for $P = X^x \cdot Z^z$ with $x, z \in \{0, 1\}$, absorbing the factor i of Y and -1 of ZX in α . The function α is injective, i.e., $\alpha(s) = \alpha(t)$ implies $s = t$, based on our earlier observations about f .

It follows that each subfunction $f_{\vec{a}}$ requires a separate node at level 1. So there are $\Omega(2^{n-1})$ nodes. \square

Lemma 5. There is a family of quantum states with polynomial-size MPS but exponential-size LIMDD.

Proof. MPS require only bond dimension 2 to represent the state $|\text{Sum}\rangle$. Namely, $|\text{Sum}\rangle$ is the sum of two product states. Product states always have bond dimension 1; and the sum of two states which have bond dimensions d_1 and d_2 , has bond dimension at most $d_1 + d_2$, as shown by Lem. 34.

Concretely, an MPS A with bond dimension 2 for $|\text{Sum}\rangle$ is given by

$$A_1^{x_1} = [1 \quad f_1(x_1)], \quad A_j^{x_j} = \begin{bmatrix} 1 & 0 \\ 0 & \prod_{j=2}^{n-1} f_j(x_j) \end{bmatrix} \text{ for } j = 2, 3, \dots, n-1, \quad A_n^{x_n} = \begin{bmatrix} 1 \\ f_n(x_n) \end{bmatrix}, \quad (7)$$

where $x_1, x_2, \dots, x_n \in \{0, 1\}$ and f_j is the function $\{0, 1\} \rightarrow \mathbb{C}$ defined by $f_j(0) = 1$ and $f_j(1) = e^{i\pi 2^{-j-1}}$. Some computation shows that, indeed, $A_1^{x_1} \cdot \dots \cdot A_n^{x_n} = (1 + \prod_{j=1}^n f_j(x_j)) = 1 + e^{i\pi(x)2^{2^{-n-1}}} = \langle x | \text{Sum} \rangle$, as desired. Moreover, the bond dimension of the MPS A is 2.

However, Lem. 4 shows that LIMDDs require exponential size to represent the same state. \square

Lemma 6. There is a family of quantum states with polynomial-size LIMDD but exponential-size MPS.

Proof. LIMDD can efficiently represent any stabilizer state, but some stabilizer states require exponential-size MPS (in particular, the cluster state, among others (Vinkhuijzen et al. 2023a)). \square

Lemma 7. MPS is at least as succinct as SLDD_\times .

Proof. App. D.4 provides a polynomial time transformation from SLDD_\times to MPS. \square

For proving the separation between RBM and ADD, we use the seminal Boolean function $IP : \{0, 1\}^n \rightarrow \{0, 1\}$, $\vec{x} \mapsto \sum_{k=1}^{n/2} x_k x_{k+n/2} \pmod 2$ for even n , which computes the inner product between the first half of the input with the second half. (Martens et al. 2013) show that any RBM requires a number of hidden weights m which is necessarily exponential in n .

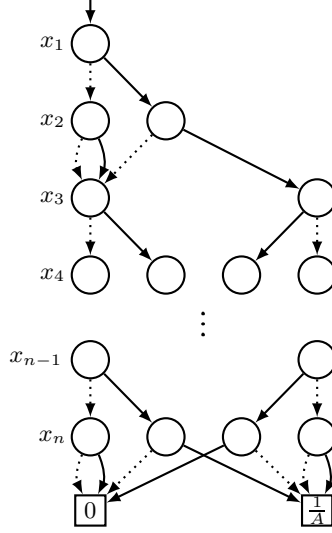


Figure 7: An ADD for the inner product function IP' from Lem. 8 made up of stacked blocks, each consisting of a layer of 2 nodes and a layer of 4 nodes. A in the right leaf is the normalization constant from Lem. 8.

Lemma 8. There is a quantum state that has linear representation both as ADD, and $SLDD_{\times}$, and LIMDD, and MPS, but requires exponential space when represented as RBM under any qubit order.

Proof. We will give the proof for the ADD; the result will then follow for $SLDD_{\times}$, LIMDD and MPS, since these are at least as succinct as ADD.

Since we consider the representation size under any qubit variable order, we may as well interleave the order. That is, we consider IP' which equals IP with x_{k+1} and $x_{k+n/2}$ swapped, i.e. $IP'(x) = x_1x_2 + x_3x_4 + \dots + x_{n-1}x_n$. Consider the n -qubit quantum state $|\varphi\rangle$ where $\langle x|\varphi\rangle = IP'(x)/A$ for $x \in \{0, 1\}$, where the normalization factor $A = \sqrt{\sum_{x \in \{0,1\}} IP'(x)}$. (Martens et al. 2013) show that any RBM requires a number of hidden weights m which is necessarily exponential in m .

There exists an ADD which represents $|\varphi\rangle$ in $O(n)$ space. This ADD is constructed from stacked blocks of two layers (of 2 and 4 nodes, respectively). The $(k+1)/2$ -th block (counting from 1 from the top) for odd $k = 1, 3, 5, \dots$ corresponds to computing the value $x_k \cdot x_{k+1}$ and adding it to the running value of $IP'(x_1, x_2, \dots, x_{k-1})$. See Fig. 7. \square

Lemma 9. RBM can represent the state $|\text{Sum}\rangle$ with a single hidden node.

Proof. All nodes have bias 0, i.e., $\beta = [0]$ and $\alpha = [0, \dots, 0]^T$ (a length- n vector). The weight on the edge between the hidden node and the j -th visible node is $e^{i\pi 2^{-j-1}}$. Then the RBM is defined by the multiplicative term of this hidden node, yielding

$$\psi(\vec{x}) = 1 + e^{w \cdot \vec{x}} = 1 + \prod_{j=1}^n e^{x_j i\pi 2^{-j-1}} \quad (8)$$

This corresponds exactly with the sum state: $|\psi\rangle = |\text{Sum}\rangle$. \square

Lemma 10. There is a state with a RBM of size $O(n)$ but which requires LIMDD of size $2^{\Theta(n)}$, for every variable order.

Proof. RBM can represent the state $|\text{Sum}\rangle$, by Lem. 9. However, Lem. 4 shows that LIMDDs require exponential size to represent this state. \square

Lemma 11. There is a family of states with polynomial-size RBM but exponential-size MPS.

Proof. RBM can efficiently represent stabilizer states, as shown by (Zhang et al. 2018). (Vinkhuijzen et al. 2023a) show that some stabilizer states require exponential-size MPS (in particular, the cluster state, among others). \square

C Proofs of Sec. 4

In this appendix, we prove Th. 2 and Th. 3 from Sec. 4.

Th. 2 is restated below. The proofs are organized per row of the table, so there is one section for each data structure. App. A contains relevant preliminaries on quantum information and QDDs.

Theorem 2. The tractability results in Table 2 hold.

We restate the other main result Th. 3 here and provide a proof.

Theorem 3. Assuming the exponential time hypothesis, the fidelity of two states represented as LIMDDs or RBMs cannot be computed in polynomial time. The proof uses a reduction from the #EVEN SUBGRAPHS problem (Jerrum and Meeks 2017).

Proof. Lem. 30 proves that LIMDD does not admit a polynomial time algorithm unless the exponential time hypothesis fails. Cor. 37 concludes the same for RBM. \square

C.1 Easy and hard operations for ADD

As noted in Sec. 2.2, the decision diagrams are special cases of each other. In particular, ADD specializes SLDD_\times , which specializes LIMDD. From this, it immediately follows that $\text{LIMDD} \preceq_s \text{SLDD}_\times \preceq_s \text{ADD}$. We also use this fact in the below proofs.

Lemma 12. ADD supports **Sample** and **Measure**.

Proof. Since ADD specializes LIMDD (see Lem. 26). \square

Lemma 13. ADD supports inner-product $\langle \varphi | \psi \rangle$.

Proof. Since ADD is a specialization of SLDD_\times (see Lem. 17). \square

Lemma 14. ADD supports **Addition** and **Equal**.

Proof. See (Fargier et al. 2014) Table 1 (EQ) and Table 2 (+BC). \square

Lemma 15. ADD supports **Local**, and hence also **Hadamard**, **X,Y,Z**, **T**, **Swap** and **CZ**.

Proof. Suppose U is a local gate on k qubits. Then U can be expressed as the sum of 4^k terms, $U = \sum_{x,y \in \{0,1\}^k} a_{xy} |x\rangle \langle y| \otimes \mathbb{I}_{n-k}$. Each of these terms individually can be applied to an ADD in polynomial time ((Fargier et al. 2014) Table 1 **CD**), since they are projections, followed by X gates. Since a constant number of states can be added in polynomial time in ADDs (Lem. 14), the result can be computed in polynomial time. Since ADD supports arbitrary k -local gates, in particular it supports all other gates that are mentioned: $H, X, Y, Z, T, \text{Swap}, \text{CZ}$. \square

Table 3: Tractability of queries and manipulations on the data structures analyzed in this paper (single application of the operation). A \checkmark means the data structure supports the operation in polytime, a \checkmark means supported in randomized polytime, and \times means the data structure does not support the operation in polytime. A \circ means the operation is not supported in polytime unless $P = NP$. ? means unknown. The table only considers deterministic algorithms (for some ? a probabilistic algorithm exists, e.g., for **InnerProd** on RBM). Novel results are blue and underlined.

	Queries					Manipulation operations						
	Sample	Measure	Equal	InnerProd	Fidelity	Addition	Hadamard	X,Y,Z	CZ	Swap	Local	T-gate
Vector	\checkmark	\checkmark	\checkmark	\checkmark	\checkmark	\checkmark	\checkmark	\checkmark	\checkmark	\checkmark	\checkmark	\checkmark
ADD App. C.1	\checkmark	\checkmark	\checkmark	\checkmark	\checkmark	\checkmark	\checkmark	\checkmark	\checkmark	\checkmark	\checkmark	\checkmark
SLDD_\times App. C.2	\checkmark	\checkmark	\checkmark	\checkmark	\checkmark	\times	\times	\checkmark	\checkmark	\times	\times	\checkmark
LIMDD App. C.3	\checkmark	\checkmark	\checkmark	\circ	\circ	\times	\times	\checkmark	\checkmark	\times	\times	\checkmark
MPS App. C.4	\checkmark	\checkmark	\checkmark	\checkmark	\checkmark	\checkmark	\checkmark	\checkmark	\checkmark	\checkmark	\checkmark	\checkmark
RBM App. C.5	\checkmark	?	?	\circ	\circ	?	?	\checkmark	\checkmark	\checkmark	?	\checkmark

C.2 Easy and hard operations for SLDD_\times

Lemma 16. SLDD_\times supports **Equal**, **Sample** and **Measure**.

Proof. Since SLDD_\times specializes LIMDD (see Lem. 26). □

Lemma 17. SLDD_\times supports inner product (**InnerProd**) and fidelity (**Fidelity**).

Proof. We show in App. D.4 that a SLDD_\times can be efficiently and exactly translated to an MPS. Since MPS supports inner product and fidelity, the result follows. □

Lemma 18. SLDD_\times does not support **Addition** in polynomial time.

Proof. (Fargier et al. 2014) (Thm. 4.9) show that **Addition** is hard for SLDD_\times . □

Lemma 19. SLDD_\times does not support **Hadamard** in polynomial time and hence neither **Local**.

Proof. By reduction from addition: Take a SLDD_\times root node v with left child a and right child b , then **Hadamard**(v) = $H|v\rangle$ is a new node with a left child $|a\rangle + |b\rangle$. By choosing $|a\rangle, |b\rangle$ to be the states from Fargier et al.'s proof showing that addition is intractable for QMDDs, the state $|a\rangle + |b\rangle$ requires an exponential-size SLDD_\times . Since SLDD_\times does not support the Hadamard gate, neither does it support arbitrary local gates (**Local**). □

Lemma 20. SLDD_\times supports Pauli gates **X,Y,Z** and **T** in polynomial time.

Proof. We will show that we can apply any single-qubit diagonal or anti-diagonal operator $A = \begin{bmatrix} \alpha & 0 \\ 0 & \beta \end{bmatrix}$ to an SLDD_\times in polynomial time. The result then immediately follows for the special cases of the gates X, Y, Z and T . Applying any diagonal local operator $A = \begin{bmatrix} \alpha & 0 \\ 0 & \beta \end{bmatrix}$ to the top qubit is easy: simply multiply the weights of the low and high edges of the diagram's root node with respectively α and β . For the anti-diagonal operator A^T , we also swap low with high edges. To apply the local operator on any qubit, simply do the above for all nodes on the corresponding level.

To see that the resulting SLDD_\times indeed represents the state $A \cdot |\psi\rangle$ (or $A^T |\psi\rangle$), consider the amplitude of any basis state $x \in \{0, 1\}^n$. The amplitude of $|x\rangle$ in an SLDD_\times is the product of the labels found on the edges while traversing the diagram from root to leaf. In the new diagram, only the weights have changed, whereas the topology has remained the same. If $x_k = 0$ (resp. $x_k = 1$), then, the k -th edge encountered during this traversal is the same in the new diagram as in the old diagram, but the label has been multiplied by α . Otherwise, if $x_k = 1$ (resp. $x_k = 0$), then the label is multiplied by β . All the other weights remain the same. Therefore, the amplitude of x in the new diagram is equal to the old amplitude multiplied by α (resp. β). □

Lemma 21. SLDD_\times supports controlled- Z in polynomial time.

Proof. Alg. 1 applies a controlled- Z gate to a SLDD_\times in time linear in the number of nodes in the SLDD_\times . To show that this is the runtime, we consider the number of times the algorithms **APPLYCONTROLLEDZ** and **APPLYZ** are called.

For both these algorithms, say that a call is *trivial* if the result is already in the cache, otherwise a call is *non-trivial*. Then a trivial call completes in constant time (i.e., in time $\mathcal{O}(1)$). Moreover, the number of trivial calls is at most twice the number of non-trivial calls. Therefore, for the purposes of obtaining an asymptotic upper bound on the running time, it suffices to count the number of non-trivial calls to the algorithm.

Thanks to the cache, a given setting of the input parameters (v, a, b) (or (v, t) in the case of **APPLYZ**) will trigger only one non-trivial call. Therefore, the number of non-trivial calls is equal to the number of distinct input parameters. But here only v varies, so the number of non-trivial calls is at most the number of nodes in the SLDD_\times . This reasoning holds for both algorithms **APPLYCONTROLLEDZ** and **APPLYZ**. Therefore, both subroutines run in time $\mathcal{O}(m)$, for an SLDD_\times which contains m nodes.

The correctness of this algorithm follows from the fact that $CZ_{a,b}|v\rangle = \lambda_0|v_0\rangle + \lambda_1 Z_b|v_1\rangle$ where node v represents an a -qubit state $\textcircled{v_0} \xrightarrow{\lambda_0} \dots \textcircled{v}$ and Z_b means applying the Z gate to the b -th qubit. This behavior is implemented by line 4. By linearity, the algorithm is correct for nodes representing k -qubit states with $k > a$. This is implemented by line 5. □

Algorithm 1: Applies a controlled- Z gate to a SLDD_\times node v , with control qubit a and target qubit b . More specifically, given a SLDD_\times node v , representing the state $|v\rangle$, this subroutine returns a SLDD_\times edge e representing $|e\rangle = CZ_a^b|v\rangle$. We assume wlog that $a > b$, since $CZ_a^b = CZ_b^a$. Here idx denotes the index of the qubit of v , and CACHE denotes a hashmap which maps triples to SLDD_\times nodes. The subroutine APPLYZ applies a Z gate to a given target qubit t .

```

1: procedure APPLYCONTROLLEDZ( $\text{SLDD}_\times$  node  $v$ , qubit indices  $a, b$ )
2:   Say that node  $v$  is  $(v_0 \xrightarrow{\lambda_0} \dots \xrightarrow{\lambda_0} v \xrightarrow{\lambda_1} v_1)$ 
3:   if the  $\text{CACHE}$  contains the tuple  $(v, a, b)$  then return  $\text{CACHE}[v, a, b]$ 
4:   else if  $\text{idx}(v) = a$  then  $r := \text{MAKENODE}(\xrightarrow{\lambda_0} v_0, \lambda_1 \cdot \text{APPLYZ}(v_1, b))$ 
5:   else  $r := \text{MAKENODE}(\lambda_0 \cdot \text{APPLYCZ}(v_0, a, b), \lambda_1 \cdot \text{APPLYCZ}(v_1, a, b))$ 
6:    $\text{CACHE}[v, a, b] := r$ 
7:   return  $r$ 
8: procedure APPLYZ( $\text{SLDD}_\times$  node  $v$ , qubit index  $t$ )
9:   Say that node  $v$  is  $(v_0 \xrightarrow{\lambda_0} \dots \xrightarrow{\lambda_0} v \xrightarrow{\lambda_1} v_1)$ 
10:  if the  $\text{CACHE}$  contains the tuple  $(v, t)$  then return  $\text{Z-CACHE}[v, t]$ 
11:  else if  $\text{idx}(v) = t$  then  $r := \text{MAKENODE}(\xrightarrow{\lambda_0} v_0, \xrightarrow{-\lambda_1} v_1)$ 
12:  else  $r := \text{MAKENODE}(\lambda_0 \cdot \text{APPLYZ}(v_0, t), \lambda_1 \cdot \text{APPLYZ}(v_1, t))$ 
13:   $\text{Z-CACHE}[v, t] := r$ 
14:  return  $r$ 

```

To prove that a single swap operation can explode the LIMDD or SLDD_\times , we first provide two lemmas.

Lemma 22. For $n \geq 1$, let $|Rot^n\rangle = \bigotimes_{j=1}^n (|0\rangle + e^{i\pi 2^{-j-1}} |1\rangle)$ and $|+^n\rangle = |+\rangle^{\otimes n}$. Then the states $|Rot^n\rangle$ and $|+^n\rangle$ have a linear-size SLDD_\times .

Proof. Fig. 8 provides the SLDD_\times representing both states. \square

Lemma 23. The following state has large LIMDD, for any variable order in which the qubit in register B comes after the qubits in register A .

$$|Sum'\rangle = |+\rangle_A^{\otimes n} |0\rangle_B + \bigotimes_{j=1}^n (|0\rangle_A + e^{i\pi 2^{-j-1}} |1\rangle_A) \otimes |1\rangle_B \quad (9)$$

Proof. The proof is similar to that of Lem. 4 except that we reason about level 2. \square

Lemma 24. SLDD_\times does not support **Swap** in polynomial time.

Proof. Let $|+^n\rangle$ and $|Rot^n\rangle$ be the states from Lem. 22, and define the following state $|\rho\rangle$ on $n+2$ qubits,

$$|\rho\rangle = |0\rangle |+\rangle |0\rangle + |1\rangle |Rot^n\rangle |0\rangle \quad (10)$$

Then $|\rho\rangle$ has a small SLDD_\times , of only size $\mathcal{O}(n)$. When we swap the first and last qubits, we obtain a state that includes $|Sum'\rangle$ from Lem. 23:

$$\text{Swap}_1^n \cdot |\rho\rangle = |0\rangle \otimes (|+\rangle |0\rangle + |Rot^n\rangle |1\rangle) \quad (11)$$

The SLDD_\times of $\text{Swap}_1^n \cdot |\rho\rangle$ is at least as large as that of $|Sum'\rangle$: First, (Wegener 2000) Th. 2.4.1 shows that constraining can never increase the DD size, so we can discard the $|0\rangle \otimes$ part (regardless of variable order), as $\text{Swap}_1^n \cdot |\rho\rangle$ is at least as large as $|Sum'\rangle$. Then Lem. 23 shows that this LIMDD has size at least $2^{\Omega(n)}$ for any variable order. Since, LIMDD is at least as succinct as SLDD_\times (see Fig. 2), this also holds for SLDD_\times . \square

Lemma 25. SLDD_\times does not support **Local** in polynomial time.

Proof. This is implied by Lem. 24. \square

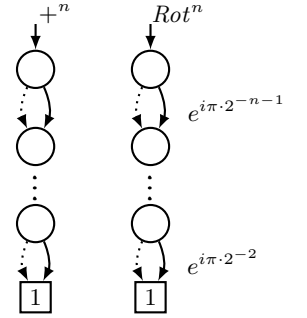


Figure 8: The states $|+^n\rangle$ and $|Rot^n\rangle$ state as SLDD_\times .

C.3 Easy and hard operations for LIMDD

Lemma 26. LIMDD supports **Sample, Measure, Equal** and **X,Y,Z**.

Proof. Vinkhuijzen et al. (Vinkhuijzen et al. 2023a) show that LIMDD supports **Sample, Measure, Equal** and **X,Y,Z**. \square

Here we show that LIMDD also support applying a T gate, but does not support **Addition, H** and **Swap**. In this work, we show that computing the fidelity (and hence the inner product, as we can reduce fidelity to inner product) between two states represented by LIMDDs is NP-hard.

Lemma 27. LIMDD supports Controlled- Z in polynomial time.

Proof. Vinkhuijzen et al. (Vinkhuijzen et al. 2023a) show how to apply any controlled Pauli gate to a state represented by a LIMDD in polynomial time, in the case where the target qubit comes after the control qubit in the variable order of that LIMDD. However, in the case of the controlled- Z , there is no distinction between control and target qubit, since the gate is symmetric. Therefore, their analysis applies to all controlled- Z gates. In fact, inspecting their method, we see that the LIMDD of the resulting state is never larger in size than the LIMDD we started with. \square

It is known that addition is hard for SLDD_\times (see Table 2 in (Fargier et al. 2014)). For LIMDD, the same was suspected, but not proved in (Vinkhuijzen et al. 2023a). We show it here by showing that $\langle Z \rangle$ -LIMDD does not support addition in polytime.

Lemma 28. LIMDD does not support **Addition** in polytime.

Proof. Consider the states $|+^n\rangle$ and $|Rot^n\rangle$ as defined in Lem. 23. Both states have polynomially sized QMDDs as shown in Lem. 22. Since LIMDD is at least as succinct as SLDD_\times (see Fig. 2), the LIMDDs representing these states are also small. However, their sum is the state $|Sum\rangle = |+^n\rangle + |Rot^n\rangle$, which has an exponential-size LIMDD relative to every variable order by Lem. 4. \square

Lemma 29. LIMDD does not support **Hadamard** in polynomial time, and hence neither does it support **Local**.

Proof. Since Hadamard can be used together with measurement (called *conditioning* by Fargier (Fargier et al. 2014)) to realize state addition as explained in Sec. 4, it is also intractable. (Recall also from (Wegener 2000) Th. 2.4.1 that conditioning never increases DD size; this is true in particular for LIMDDs) \square

We now prove that the fidelity of LIMDDs cannot be computed in polynomial time, under common assumptions of complexity theory.

LIMDD FIDELITY is hard to compute. We show that LIMDD FIDELITY cannot be computed in polynomial time, unless the Exponential Time Hypothesis (ETH) is false. This proof implies that inner product is hard, since fidelity reduces to inner product. Proving hardness of inner product is also a specialized case of the below construction, which does not require our newly defined EOSD problem (see below) but only the well-known hard problem of counting even subgraphs of a certain size ($\#\text{EVEN SUBGRAPHS}$).

The proof of LIMDD FIDELITY hardness proceeds in several steps. The starting point is Jerrum and Meeks' result that the problem $\#\text{EVEN SUBGRAPHS}$ cannot be solved in polynomial time unless ETH is false (Lem. 30). We introduce a problem we call $\text{EVEN ODD SUBGRAPHS DIFFERENCE}$ (EOSD). We give a reduction from $\#\text{EVEN SUBGRAPHS}$ to EOSD, thus showing that EOSD cannot be solved in polynomial time, under the same assumptions (Lem. 32). This step is the most technical part of the proof. Finally, we give a reduction from EOSD to LIMDD FIDELITY, thus obtaining the desired result, that LIMDD FIDELITY cannot be computed in polynomial time (to a certain precision), unless ETH is false (Lem. 31). In this step, we use the fact that LIMDDs can efficiently represent Dicke states and graph states (a type of stabilizer state). Specifically, we will show that computing the fidelity between these states essentially amounts to solving EOSD for the given graph state. Dicke states were first studied by (Dicke 1954); see also (Bärtschi and Eidenbenz 2019).

We first formally define the three problems above, including computing the fidelity of two LIMDDs. We will need the following terminology for graphs. For an undirected graph $G = (V, E)$ and a set of vertices $S \subseteq V$, we denote by $G[S]$ the subgraph induced by S . If $|S| = k$, then we say that $G[S]$ is a k -induced subgraph, and we say that it is an *even* (resp. *odd*) subgraph if $G[S]$ has an even (resp. odd) number of edges. We let $e(G, k)$ (resp. $o(G, k)$) denote the number of even (resp. odd) k -induced subgraphs of G .

LIMDD FIDELITY.

Input: Two LIMDDs, representing the states $|\varphi\rangle, |\psi\rangle$

Output: The value $|\langle\varphi|\psi\rangle|^2$ to $2n$ bits of precision.

#EVEN SUBGRAPHS

Input: A graph $G = (V, E)$, and an integer k

Output: The value $e(G, k)$.

EVEN ODD SUBGRAPH DIFFERENCE (EOSD).

Input: A graph $G = (V, E)$, and an integer k .

Output: The value $|e(G, k) - o(G, k)|$, i.e., the absolute value of the difference between the number of even and odd induced k -subgraphs of G .

Lemma 30 ((Jerrum and Meeks 2017)). If #EVEN SUBGRAPHS is polytime, then ETH is false.

Proof. (Jerrum and Meeks 2017) showed that counting the number of even induced subgraphs with k vertices is #W[1]-hard. Consequently, there is no algorithm running in time $poly(n)$ (independent of k) unless the exponential time hypothesis fails. \square

Lemma 31. There is no polynomial-time algorithm for LIMDD FIDELITY, i.e., for computing fidelity between two LIMDDs to $2n$ bits of precision, unless the Exponential Time Hypothesis (ETH) fails.

Proof. Suppose there was such a polynomial-time algorithm, running in time $O(n^c)$ for some constant $c \geq 1$. We will show that then EOSD can be solved in time $O(n^c)$ (independent of k), by giving a reduction from EOSD to LIMDD FIDELITY. From Lem. 32, it would then follow that ETH is false.

The reduction from EOSD to LIMDD FIDELITY is as follows.

Let G be an input graph on n vertices V and $0 \leq k \leq n$ an integer. Let $|G\rangle$ be the graph state corresponding to G (Van den Nest, Dehaene, and De Moor 2004), so that

$$|G\rangle = \frac{1}{2^{n/2}} \sum_{S \subseteq V} (-1)^{|G[S]|} |S\rangle \quad (12)$$

where $|G[S]|$ denotes the number of edges in the S -induced subgraph of G , and $|S\rangle$ denotes the computational-basis state $|S\rangle = |x_1\rangle \otimes |x_2\rangle \otimes \dots \otimes |x_n\rangle$ with $x_j = 1$ if $j \in S$ and $x_j = 0$ otherwise. Let $|D_n^k\rangle$ be the Dicke state (Dicke 1954).

$$|D_n^k\rangle = \frac{1}{\sqrt{\binom{n}{k}}} \sum_{\vec{x} \in \{0,1\}^n \text{ with } |\vec{x}|=k} |\vec{x}\rangle \quad (13)$$

Both these states have small LIMDDs:

Dicke state (Bryant 1986) gives a construction for BDDs to represent the function $f_k : \{0, 1\}^n \rightarrow \{0, 1\}$, with $f_k(x) = 1$ iff $|x| = k$. This is precisely the amplitude function of the Dicke state $|D_n^k\rangle$ (up to a factor $1/\sqrt{\binom{n}{k}}$). This construction also works for LIMDDs, by simply setting all the edge labels to the identity, and using root label $1/\sqrt{\binom{n}{k}} \cdot \mathbb{I}^{\otimes n}$.

Graph state (Vinkhuijzen et al. 2023a) show how to efficiently construct a LIMDD for any graph state.

It is straightforward to verify that the fidelity between $|D_n^k\rangle$ and $|G\rangle$ is related to the subgraphs of G , as follows,

$$\langle D_n^k | G \rangle = \frac{1}{\sqrt{\binom{n}{k}} 2^n} \sum_{S \subseteq V: |S|=k} (-1)^{|G[S]|} = \frac{1}{\sqrt{\binom{n}{k}} 2^n} (e(G, k) - o(G, k)) \quad (14)$$

Hence,

$$\underbrace{|e(G, k) - o(G, k)|}_{\text{solution to EOSD}} = \sqrt{\binom{n}{k} 2^n} \underbrace{|\langle D_n^k | G \rangle|^2}_{\text{Fidelity}} \quad (15)$$

Since $|\langle D_n^k | G \rangle|^2$ denotes the fidelity between $|D_n^k\rangle$ and $|G\rangle$, and $|e(G, k) - o(G, k)|$ denotes the quantity asked for by the EOSD problem, this completes the reduction. The overhead of constructing the LIMDDs from the description of the Dicke and graph states takes linear time in the size of the resulting LIMDD. So, if the fidelity of two LIMDDs is computed in polynomial

time, say, in time $\mathcal{O}(n^c)$, then also the quantity $|e(G, k) - o(G, k)|$ is computed in time $\mathcal{O}(n^c)$; thus, EOSD is solved in time $\mathcal{O}(n^c)$. Lastly, we address the number of bits of precision required. In order to exactly compute the integer $|e(G, k) - o(G, k)|$, it is necessary to compute the fidelity $|\langle D_n^k | G \rangle|^2$ with a precision of at least one part in $\binom{n}{k} 2^n$. Put another way, the required number of bits of precision is $\log_2(\binom{n}{k} \cdot 2^n) \leq \log_2(2^n \cdot 2^n) = 2n$. Summarizing, computing the fidelity of (the states represented by) two LIMDDs representing a graph state and a Dicke state, to $2n$ bits of precision, is not possible in polynomial time, unless ETH fails. \square

Lemma 32. There is no polynomial-time algorithm for EOSD, unless ETH is false.

Proof. We provide an efficient reduction (in Alg. 2) from #EVEN SUBGRAPHS: the problem, on input an undirected graph G and a parameter $k \in \{0, 1, 2, \dots, |V|\}$, of computing the number of k -vertex induced subgraphs which have an even number of edges. It follows that, if EOSD can be computed in polynomial time, then Alg. 2, which computes #EVEN SUBGRAPHS, also runs in polynomial time. Jerrum and Meeks (Jerrum and Meeks 2017) show that #EVEN-SUBGRAPHS cannot be computed in polynomial time unless ETH is false (Lem. 30). Therefore, if EOSD could be computed in polynomial time, then ETH would be false.

The algorithm COUNT-EVEN-SUBGRAPHS (Alg. 2) takes as parameters a graph G and an integer $k \geq 0$, and outputs $e(G, k)$, the number of even k -induced subgraphs of G , thus solving #EVEN SUBGRAPHS. This algorithm uses at most $2n$ invocations of a subroutine EVEN-ODD-SUBGRAPHS-DIFFERENCE; therefore, if the subroutine EVEN-ODD-SUBGRAPHS-DIFFERENCE runs in polynomial time, then so does COUNT-EVEN-SUBGRAPHS.

Let us briefly sketch the idea behind the algorithm, before we give a formal proof of correctness. First, we know that $e(G, k) + o(G, k) = \binom{n}{k}$, since each subgraph is either even or odd, and G has $\binom{n}{k}$ different k -induced subgraphs in total. Thus, if we knew the (possibly negative) difference $\zeta_k = e(G, k) - o(G, k)$, then we know the sum and difference of $e(G, k)$ and $o(G, k)$, so we could compute the desired value $e(G, k) = \frac{1}{2}(\binom{n}{k} + \zeta_k)$. Unfortunately, EVEN-ODD-SUBGRAPHS-DIFFERENCE only tells us the absolute value, $|\zeta_k|$. Fortunately, we know that $e(G, 0) = 1$ and $o(G, 0) = 0$, so $\zeta_0 = 1 - 0 = 1$ (namely, there is only one induced subgraph with 0 vertices, and it has 0 edges, which is even). We now bootstrap our way up, computing ζ_j for $j = 1, \dots, k$ using the previously known results. The key ingredient is that, by adding isolated vertices to the graph and querying EVEN-ODD-SUBGRAPHS-DIFFERENCE on this new graph, we can discover the absolute difference $|\zeta_j + \zeta_{j-1}|$, which allows us to compute the values ζ_j .

Correctness of the algorithm. We now prove that the algorithm COUNT-EVEN-SUBGRAPHS outputs the correct value. Let (G, k) be the input to the algorithm. For $j = 0, \dots, k$, let $\zeta_j = e(G, j) - o(G, j)$. We will show that, for each $j = 1, \dots, k$, the algorithm sets the variable d_j to the value ζ_j in the j -th iteration of the for-loop. The proof is by induction on j . In the induction hypothesis, we include also that the variable ℓ is always the largest value below j satisfying $\zeta_\ell \neq 0$ as in Eq. (16) (this value is well-defined, since $1 = \zeta_0 \neq 0$, so we have $0 \leq \ell < j$).

$$\ell = \max\{0 \leq \ell < j \mid \zeta_\ell \neq 0\} \quad (16)$$

Algorithm 2: An algorithm which computes the number of even k -induced subgraphs using at most $2n$ calls to a subroutine EVEN-ODD-SUBGRAPHS-DIFFERENCE, which returns $|e(G, k) - o(G, k)|$ on input (G, k) .

```

1: procedure COUNT-EVEN-SUBGRAPHS( $G = (V, E), k$ )
   Output: The number of even induced subgraphs of  $G$  with  $k$  vertices
2:    $d_0 := 1$  ▷  $d$  is an array of  $k + 1$  integers
3:    $\ell := 0$  ▷ Last iteration when  $\zeta_j = 1$ 
4:   for  $j := 1, \dots, k$  do
5:      $q :=$  EVEN-ODD-SUBGRAPHS-DIFFERENCE( $G, j$ )
6:     if  $q = 0$  then ▷ There are equally many even as odd subgraphs
7:        $d_j := 0$ 
8:     else ▷ Else we have to figure out whether there more even or odd subgraphs:
9:        $G' := (V \cup \{v'_1, \dots, v'_{j-\ell}\}, E)$  ▷ Add  $j - \ell$  new isolated vertices
10:       $p :=$  EVEN-ODD-SUBGRAPHS-DIFFERENCE( $G', j$ )
11:       $d_j := \begin{cases} q & \text{if } |d_\ell + q| = p \\ -q & \text{if } |d_\ell - q| = p \end{cases}$ 
12:       $\ell := j$  ▷ Since iteration  $j$  is the latest iteration having  $\zeta_j = 1$ 
13:   return  $\frac{1}{2}(\binom{n}{k} + d_k)$ 

```

For the base case, where $j = 0$, it suffices to note that there is only one set with zero vertices – the empty set – which induces the empty graph, which contains an even number of edges. Therefore, $\zeta_0 = 1$, which the algorithm sets on line 2. Finally, ℓ is correctly set to 0.

For the induction case $j \geq 1$, the variables d_t have been set to $d_t = \zeta_t$ for $t = 0, \dots, j-1$ and ℓ satisfies Eq. (16) from the induction hypothesis. Consequently, we have $\zeta_{\ell+1} = \dots = \zeta_{j-1} = 0$. If $\zeta_j = 0$, then the algorithm sets $q := |\zeta_j| = |0| = 0$ on line 5, so the algorithm sets d_j correctly on line 7, and correctly leaves ℓ untouched (ℓ remains unchanged from the $j-1$ -th to the j -th iteration). Otherwise, if $\zeta_j \neq 0$, the algorithm adds $j - \ell$ new, isolated vertices to G , obtaining the new graph $G' = (V_G \cup \{v'_1, \dots, v'_{j-\ell}\}, E_G)$. On line 10, it computes the value $|e(G', j) - o(G', j)|$ of this graph. Since this expression also sums over induced subgraphs of G' that contain isolated vertices, this value can be expressed as follows:

$$p := |e(G', j) - o(G', j)| \quad (17)$$

$$= \left| \sum_{a=\ell}^j \binom{j-\ell}{j-a} (e(G, a) - o(G, a)) \right| = \left| \sum_{a=\ell}^j \binom{j-\ell}{j-a} \zeta_a \right| \quad (18)$$

$$= \left| \binom{j-\ell}{j-\ell} \zeta_\ell + \binom{j-\ell}{0} \zeta_j \right| = |\zeta_\ell + \zeta_j| \quad (19)$$

We noted that $\zeta_{\ell+1} = \dots = \zeta_{j-1} = 0$; therefore, these terms vanish from the summation (step from Eq. (18) to Eq. (19)), so that only $p = |\zeta_j + \zeta_\ell|$ remains. Since we now know the values of $\zeta_\ell, |\zeta_j|$ and $|\zeta_j + \zeta_\ell|$ and since $\zeta_\ell \neq 0$, we can infer the value of ζ_j , which is done on line 11. We conclude that each variable d_j is correctly set to ζ_j , concluding the proof by induction. Also, since $\zeta_j \neq 0$, ℓ is correctly set to j .

Lastly, we show that the value returned by the algorithm is indeed the number $e(G, k)$. Suppose that $d_k = \zeta_k = e(G, k) - o(G, k)$. We know that $e(G, k) + o(G, k) = \binom{n}{k}$. That is, we know both the sum and the difference of $e(G, k), o(G, k)$; therefore we can compute them both. By adding these two equations and solving for $e(G, k)$, we obtain $e(G, k) = \frac{1}{2} (\binom{n}{k} + d_k)$, which is the value returned by the algorithm. \square

Lemma 33. LIMDD supports the T -gate.

Proof. Alg. 3 applies an arbitrary diagonal gate $D = \begin{bmatrix} \rho & 0 \\ 0 & \omega \end{bmatrix}$ to a state represented by a LIMDD. To apply a T -gate, one calls the algorithm with $D = T = \begin{bmatrix} \rho & 0 \\ 0 & e^{i\pi/4} \end{bmatrix}$. We now show that the algorithm runs in polynomial time. First, since each recursive call takes $\mathcal{O}(1)$ time, for the purposes of estimating runtime it suffices to count the number of recursive calls. The cache stores all tuples of nodes and matrices with which the algorithm is called, so for the purposes of estimating the runtime it suffices to count the number of *distinct* recursive calls. To this end, we note that the recursive calls to the algorithm only receive two different matrices, namely $\begin{bmatrix} \rho & 0 \\ 0 & \omega \end{bmatrix}$ and $\begin{bmatrix} \omega & 0 \\ 0 & \rho \end{bmatrix}$. The nodes that are passed as argument v are nodes that are already in the diagram. Therefore, if the diagram contains m nodes, then at most $2m$ distinct recursive calls are made. We conclude that the runtime is polynomial (indeed, linear), in the size of the diagram. \square

Algorithm 3: Applies a diagonal gate D to qubit k of a state represented by a LIMDD.

```

1: procedure APPLYDIAGGATE(LIMDD Node  $v = \textcircled{v_0} \xrightarrow{\lambda_0 A_0} \dots \textcircled{\dots} \xrightarrow{\lambda_1 A_1} \textcircled{v_1}$ , gate  $D$ , qubit  $k$ )
   with  $D = \begin{bmatrix} \rho & 0 \\ 0 & \omega \end{bmatrix}$ 
   Node  $v$  represents a state on  $n$  qubits
2:   if CACHE contains the tuple  $(v, D)$  then return CACHE[ $v, D$ ]
3:   else if  $k = n$  then
4:     return  $\textcircled{v_0} \xrightarrow{\rho \lambda_0 A_0} \dots \textcircled{\dots} \xrightarrow{\omega \lambda_1 A_1} \textcircled{v_1}$ 
5:   else
6:     gate  $E := \begin{bmatrix} \omega & 0 \\ 0 & \rho \end{bmatrix}$ 
7:     for  $i = 0, 1$  do
8:       gate  $F_i := \begin{cases} D & \text{if } A_i^k \in \{I, Z\} \\ E & \text{if } A_i^k \in \{X, Y\} \end{cases} \quad \triangleright \text{Here } A_i^k \text{ denotes the } k\text{-th qubit of the Pauli operator } A^i$ 
9:       Node  $u_i := \text{APPLYTGATETO LIMDD}(v_0, F_i, k)$ 
10:    Node  $r := \textcircled{u_0} \xrightarrow{\lambda_0 A_0} \dots \textcircled{\dots} \xrightarrow{\lambda_1 A_1} \textcircled{u_1}$ 
11:    CACHE[ $v, D$ ] :=  $r$ 
12:    return  $r$ 

```

C.4 Supported operations of MPS

(Vidal 2003) shows that MPS supports efficient application of a single one-qubit gate or two-qubit gate on consecutive qubits, which includes **X, Y, Z, Hadamard, T**. This extends to any two-qubit operation on any qubits (Perez-Garcia et al. 2007), particularly including **Swap** and **CZ** gates. These algorithms are extendable to k -local gates on adjacent qubits, which does not increase the largest matrix dimension D to more than D^k . The algorithm consists of merging the k tensors (the j -th tensor combines the two matrices A_j^0 and A_j^1) into a single large one, applying the gate to the large tensor, followed by splitting the tensor again into k matrices A_j^0 and A_j^1 again by use of the singular-value decomposition (for details on the merging and splitting see e.g. (Dang, Hill, and Hollenberg 2019)). The largest matrix dimension during this process does not increase above D^k . Using **Swap** gates, one thus implements **Local** on any qubits. We give a direct proof of the support for addition below (Lem. 34).

(Orús 2014) gives an accessible exposition of TN, of which MPS is a special case. He explains how to compute the inner product in polynomial time. Thus, MPS also supports **Measure**. **Sample** can be done by a Markov Chain Monte Carlo approach, invoking **Measure** as subroutine. Since inner product is supported, so is **Equal**: MPS M and M' are equivalent iff $\frac{|(M|M')|^2}{(M|M) \cdot (M'|M')} = 1$.

Lemma 34. MPS supports addition in polynomial time.

Proof. Let A, B be MPSs. Then a new MPS C representing $|C\rangle = |A\rangle + |B\rangle$ can be efficiently constructed as follows, for $x = 0, 1$ and $j = 2, \dots, n-1$:

$$C_n^x = [A_n^x \ B_n^x] \quad C_j^x = \begin{bmatrix} A_j^x & 0 \\ 0 & B_j^x \end{bmatrix} \quad C_1^x = \begin{bmatrix} A_1^x \\ B_1^x \end{bmatrix} \quad (20)$$

□

C.5 Supported operations of RBM

(Jónsson, Bauer, and Carleo 2018) show that RBM supports Pauli gates, the controlled- Z gate and the T -gate (and, in fact, arbitrary phase gates). There is at the moment no efficient exact algorithm for the **Hadamard** gate, which would make the list of supported gates universal. Hence there is at the moment no exact efficient algorithm for **Local** either. **Sample** is supported for any n -qubit RBM M , see e.g. Appendix B of (Jónsson, Bauer, and Carleo 2018) and references therein, by performing a Markov Chain Monte Carlo algorithm (e.g. Metropolis algorithm) where the Markov Chain state space consists of all bit strings $x \in \{0, 1\}^n$, and the corresponding unnormalized probability $|\langle x|M \rangle|^2$ of each state is efficiently computed using Eq. (1). No exact algorithm for **Equal** is known (in fact, the related problem of identity testing when one only has sampling access to one of the two RBMs is already computationally hard (Blanca et al. 2021)). Although no exact algorithm for **InnerProd** is known, it can be approximated using **Sample** as subroutine (see e.g. (Wu, Duan, and Deng 2020)). Furthermore, **Measure** can be approximated by computing the normalization factor $1/\langle M|M \rangle$ using the (exact or approximate) algorithm for **InnerProd**, while the relative outcome probabilities are defined in Eq. (1).

Lemma 35. RBM supports **Swap**.

Proof. In order to effect a swap between qubits q_1 and q_2 , we simply exchange rows q_1 and q_2 in the matrix W and the vector $\vec{\alpha}$, obtaining W' and $\vec{\alpha}'$. Then $\mathcal{M}' = (\vec{\alpha}', \vec{\beta}, W', m)$ has $|\mathcal{M}'\rangle = \text{SWAP}(q_1, q_2) \cdot |\mathcal{M}\rangle$. □

(Torlai et al. 2018) note that RBMs can exactly represent Dicke states. In Lem. 36, we give another construction of succinct RBMs for Dicke states, where the number of hidden nodes grows linearly with the number of visible nodes.

Lemma 36. An RBM can exactly represent any Dicke state, using only $2n$ hidden nodes.

Proof. We will construct an RBM with $2n$ hidden nodes representing $|D_n^k\rangle$.

For each $j \in \{0, 1, \dots, n\} \setminus \{k\}$, our construction will use two hidden nodes. Fix such a j . Then the first hidden node is connected to each visible node with weight $i\pi/n$, and has bias $b_j = i\pi(1 - j/n)$. The second hidden node is connected to each visible node with weight $-i\pi/n$ and has bias $b_j = -i\pi(1 - j/n)$. Since the weights on all edges incident to a given hidden node are the same, the term it contributes depends only on the weight of the input (i.e., the number of zeroes and ones). Thus, these two nodes contribute a multiplicative factor $(1 + e^{i\pi(1+|x|/n+j/n)})$ and $(1 + e^{-i\pi(1+|x|/n-j/n)})$, respectively. Multiplying these together, the two terms collectively contribute a multiplicative term of $2 + 2\cos(\pi(1+|x|/n-j/n)) = 2 - 2\cos(\pi(|x|-j)/n)$, which is 0 iff $|x| = j$ and nonzero otherwise. Let a be the constant $a = \prod_{j=0, j \neq k}^n 2 - 2\cos(\pi(k-j)/n)$, i.e., the product of

all terms when $|x| = k$. Then the RBM represents the following state unnormalized function $\Psi : \{0, 1\}^n \rightarrow \mathbb{C}$, which we then normalize to obtain the state $|\Psi\rangle$:

$$\Psi(x) = \begin{cases} a & \text{if } |x| = k \\ 0 & \text{otherwise} \end{cases} \quad |\Psi\rangle = \frac{1}{a\sqrt{\binom{n}{k}}} \sum_x \Psi(x) |x\rangle \quad (21)$$

The normalized state $|\Psi\rangle$ represents exactly the Dicke state $|D_n^k\rangle$, since its amplitudes are equal to $1/\sqrt{\binom{n}{k}}$ when $|x| = k$ and zero otherwise. \square

Since RBM can succinctly represent both Dicke states (Lem. 36) and graph states, a subset of stabilizer states (Zhang et al. 2018), the proof for hardness of LIMDD FIDELITY (Lem. 31) is also applicable to RBM.

Corollary 37. There is no polynomial-time algorithm for RBM FIDELITY, i.e., for computing fidelity between two RBM to $2n$ bits of precision, unless the Exponential Time Hypothesis (ETH) fails.

D Proofs of Sec. 5

App. D.1 proves that our rapidity definition is a preorder and is equivalent to the one given by (Lai, Liu, and Yin 2017) for canonical data structures.

App. D.2 provides the proof for the sufficient condition for rapidity and App. D.3-D.5 prove its application to the data structures studied in this paper.

D.1 Rapidity Definition

We now show that rapidity is a preorder over data structures and that the definition of (Lai, Liu, and Yin 2017) can be considered a special case for canonical data structures. For convenience, we restate the definition of rapidity.

Definition 3 (Rapidity for non-canonical data structures). Let D_1, D_2 be two data structures and consider some c -ary operation OP on these data structures. In the below, ALG_1 (ALG_2) is an algorithm implementing OP for D_1 (D_2).

- (a) We say that ALG_1 is *at most as rapid as* ALG_2 iff there exists a polynomial p such that for each input $\varphi = (\varphi_1, \dots, \varphi_c)$ there exists an equivalent input $\psi = (\psi_1, \dots, \psi_c)$, i.e., with $|\varphi_j| = |\psi_j|$ for $j = 1 \dots c$, for which $time(ALG_2, \psi) \leq p(time(ALG_1, \varphi))$. We say that ALG_2 is *at least as rapid as* ALG_1 .
- (b) We say that $OP(D_1)$ is *at most as rapid as* $OP(D_2)$ if for each algorithm ALG_1 performing $OP(D_1)$, there is an algorithm ALG_2 performing $OP(D_2)$ such that ALG_1 is at most as rapid as ALG_2 .

Theorem 4. Rapidity is a preorder over data structures.

Proof. We first show that rapidity is reflexive, next we show that it is transitive.

Rapidity is reflexive. It suffices to show that rapidity is a reflexive relation on algorithms performing a given operation. Let D be a data structure, OP an operation and ALG an algorithm performing $OP(D)$. Then ALG is at most as rapid as itself if there exists a polynomial p such that for each input φ there exists an equivalent input ψ with $time(ALG, \varphi) \leq p(ALG, \psi)$. We may choose the polynomial $p(x) = x$, and we may choose $\psi := \varphi$. Then the statement reduces to the trivial statement $time(ALG, \varphi) = time(ALG, \psi) = p(ALG, \psi)$.

Rapidity is transitive. It suffices to show that rapidity is a transitive relation on algorithms. To this end, let D_1, D_2, D_3 be data structures, OP an operation and ALG_1, ALG_2, ALG_3 algorithms performing $OP(D_1), OP(D_2), OP(D_3)$, respectively. Suppose that ALG_1 is at most as rapid as ALG_2 and ALG_2 is at most as rapid as ALG_3 . We will show that ALG_1 is at most as rapid as ALG_3 . By the assumptions above, there are polynomials p and q such that (i) for each input φ there exists an equivalent input ψ such that $time(ALG_2, \psi) \leq p(time(ALG_1, \varphi))$; and (ii) for each input ψ there exists an equivalent input γ such that $time(ALG_3, \gamma) \leq q(time(ALG_2, \psi))$.

Put together, for every input φ there exist equivalent inputs ψ and γ such that $time(ALG_3, \gamma) \leq q(time(ALG_2, \psi)) \leq q(p(time(ALG_1, \varphi)))$. Letting the polynomial $\ell(x) = q(p(x))$, we obtain that for every φ there exists an equivalent γ such that $time(ALG_3, \gamma) \leq \ell(ALG_1, \varphi)$. \square

We note that an alternative definition of rapidity (Lai, Liu, and Yin 2017), which always allows ALG_2 to read its input by requiring $\text{time}(ALG_2, y) \leq p(\text{time}(ALG_1, x) + |y|)$ instead of $\text{time}(ALG_2, y) \leq p(\text{time}(ALG_1, x))$, is not transitive for query operations:

Consider the data structure Padded $SLDD_\times$, ($PSLDD_\times$) which is just a QMDD, except that a string of 2^{2^n} "0"s have been concatenated to the end of the $SLDD_\times$ representation, where n is the number of qubits.

Under the alternative rapidity relation \geq_r^{alt} , both ADD and $SLDD_\times$ are at least as rapid as $PSLDD_\times$, because the ADD algorithm is allowed to run for $\text{poly}(2^{2^n})$ time. But $PSLDD_\times$ is also at least as rapid as $SLDD_\times$, because algorithms for $PSLDD_\times$ don't need to read the whole 2^{2^n} -length input — they only read the $SLDD_\times$ at the beginning of the string. Put together, this leads to:

$$ADD \geq_r^{\text{alt}} PSLDD_\times \geq_r^{\text{alt}} SLDD_\times \quad \text{and} \quad ADD \not\geq_r^{\text{alt}} SLDD_\times.$$

Next, we show that our definition of rapidity is equivalent to Lai et al.'s definition of rapidity in the case when both data structures are canonical and we restrict our attention to only those algorithms which run in time at least m where m is the size of the input. For convenience, we restate Lai et al.'s definition here.

Definition 6 (Rapidity for canonical data structures (Lai, Liu, and Yin 2017)). A c -ary operation OP on a canonical language L_1 is *at most as rapid as* OP on another canonical language L_2 , iff for each algorithm ALG performing OP on L_1 there exists some polynomial p and some algorithm ALG_2 performing OP on L_2 such that for every valid input $(\varphi_1, \dots, \varphi_c, \alpha)$ of OP on L_1 and every valid input $(\psi_1, \dots, \psi_c, \alpha)$ of OP on L_2 satisfying $\varphi_i \equiv \psi_i$ ($1 \leq i \leq c$), $ALG_2(\psi_1, \dots, \psi_c, \alpha)$ can be done in time $p(t + |\varphi_1| + \dots + |\varphi_c| + |\alpha|)$, where α is any element of supplementary information and t is the running time of $ALG(\varphi_1, \dots, \varphi_c, \alpha)$.

Lai et al. use several minor differences in notation. First, they speak of *valid* inputs (because they consider data structures which cannot represent all objects), whereas we do not; they use an element of supplementary information α as part of the input, whereas we omit such an element; they write $\varphi_i \equiv \psi_i$ where we write $|\varphi_i| = |\psi_i|$; lastly they speak of a *language* whereas we speak of a *data structure*. Since these differences between the notation are inconsequential, it will be convenient to rephrase the definition of Lai et al. using the notation of this paper, as follows:

Definition 7 (Rapidity of canonical data structures, rephrased). In the following, ALG_1, ALG_2 are algorithms which perform OP on canonical data structures D_1, D_2 , respectively.

- (a) An algorithm ALG_1 is *at most as rapid as* an algorithm ALG_2 iff there is a polynomial p such that for each input φ and for each equivalent input ψ , it holds that $\text{time}(ALG_2, \psi) \leq p(\text{time}(ALG_1, \varphi) + |\varphi|)$.
- (b) A canonical data structure D_1 is *at most as rapid as* a canonical data structure D_2 for an operation OP if for each algorithm ALG_1 performing OP on D_1 there is an algorithm ALG_2 performing OP on D_2 such that ALG_1 is at most as rapid as ALG_2 .

Lemma 38. Def. 3 is equivalent to the definition of (Lai, Liu, and Yin 2017) (Def. 7) in the case when two data structures D_1, D_2 are both canonical and where we restrict our attention to algorithms whose runtime is at least m , where m is the size of the input.

Proof. Let D_1, D_2 be two canonical data structures. We will show that D_1 is at most as rapid as D_2 according to Def. 3 if and only if the same is true according to Def. 7. Since items 3.(b) and 7.(b) are equivalent, it suffices to show that the two definitions are equivalent for *algorithms* rather than *data structures*. That is, we will show that an algorithm ALG_1 is at most as rapid as ALG_2 according to Def. 3 if and only if the same is true according to Def. 7.

Abusing notation, we write $|(\varphi_1, \dots, \varphi_c)|$ instead of $|\varphi_1| + \dots + |\varphi_c|$, etc. In this proof, we will assume without loss of generality that all polynomials p are monotonically increasing (i.e., $p(x) \leq p(y)$ if $x \leq y$). Namely, if p is a polynomial which does not monotonically increase, then use instead the polynomial $p'(x) = p(x) + x^k$ for sufficiently large k .

Direction if. Let ALG_1, ALG_2 be algorithms performing OP on canonical data structures D_1, D_2 , respectively, such that ALG_1 is at most as rapid as ALG_2 according to Def. 7. Then there is a polynomial p such that $\text{time}(ALG_2, \psi) \leq p(\text{time}(ALG_1, \varphi) + |\varphi|)$ for all equivalent inputs φ, ψ . Since the data structures D_1, D_2 can represent all quantum state vectors, there certainly *exists* an equivalent ψ to any φ ; indeed, since D_2 is canonical, there is a unique such instance ψ . Since we restrict our attention to algorithms with runtime at least m where m is the size of the input, we get that $|\varphi| \leq \text{time}(ALG_1, \varphi)$, so $p(\text{time}(ALG_1, \varphi) + |\varphi|) \leq p(2 \cdot \text{time}(ALG_1, \varphi))$.

Therefore, let $q(x) = p(2x)$. Now we get that, for every input φ , there exists an equivalent input ψ such that $\text{time}(ALG_2, \psi) \leq q(\text{time}(ALG_1, \varphi))$. Therefore, ALG_1 is at most as rapid as ALG_2 according to Def. 3.

Direction only if. Suppose that ALG_1 is at most as rapid as ALG_2 according to Def. 3. Then there is a polynomial p such that for each input φ , there is an equivalent input ψ such that $time(ALG_2, \psi) \leq p(time(ALG_1, \varphi))$. Using the monotonicity of p which we assume without loss of generality, we get that $p(time(ALG_1, \varphi)) \leq p(time(ALG_1, \varphi) + |\varphi|)$. Lastly, since D_2 is canonical, any instance ψ which is equivalent to φ must be the *only* input instance that is equivalent to φ . Therefore, we obtain that there exists a polynomial p such that for each input φ and for all equivalent inputs ψ (i.e., for the unique equivalent instance ψ of D_2), it holds that $time(ALG_2, \psi) \leq p(time(ALG_1, \varphi) + |\varphi|)$. Therefore, ALG_1 is at most as rapid as ALG_2 according to Def. 7. \square

D.2 A Sufficient Condition for Rapidity

Here, we prove Th. 5, which we restate below.

Theorem 5 (A sufficient condition for rapidity). Let D_1, D_2 be data structures with $D_1 \preceq_s D_2$ and OP a c -ary operation. Suppose that,

- A1 $OP(D_2)$ requires time $\Omega(m)$ where m is the sum of the sizes of the operands; and
- A2 for each algorithm ALG implementing $OP(D_2)$, there is a runtime monotonic algorithm ALG^{rm} , implementing the same operation $OP(D_2)$, which is at least as rapid as ALG ; and
- A3 there exists a transformation from D_1 to D_2 which is (i) weakly minimizing and (ii) runs in time polynomial in the output size (i.e, in time $\text{poly}(|\psi|)$ for transformation output $\psi \in D_2$); and
- A4 if OP is a manipulation operation (as opposed to a query), then there also exists a polynomial time transformation from D_2 to D_1 (polynomial time in the input size, i.e, in $|\rho|$ for transformation input $\rho \in D_2$).

Then D_1 is at least as rapid as D_2 for operation OP .

Proof. We prove the theorem for $c = 1$. This can be easily extended to the case with multiple operands by treating the operands point-wise and summing their sizes. We show that $OP(D_2)$ is at most as rapid as $OP(D_1)$, assuming that the conditions in Th. 5 hold. (Note that this swaps the roles of D_1 and D_2 relative to Def. 3). In this proof, we will assume without loss of generality that all polynomials p are monotone, i.e., if $x \leq y$ then $p(x) \leq p(y)$.

We prove the theorem for a manipulation operation OP . The proof for a query operation OP follows as a special case, which we treat at the end of the proof.

Let ALG_2 be an $\Omega(m)$ algorithm implementing $OP(D_2)$. By A2, we may assume without loss of generality that ALG_2 is runtime monotonic. Let $f: D_1 \rightarrow D_2$ be the polynomial-time weakly minimizing transformation (A3), and $g: D_2 \rightarrow D_1$ the polynomial-time transformation in the other direction satisfying the criteria in A4.

We set $ALG_1 = f \circ ALG_2 \circ g$, i.e., ALG_1 is as follows.

```

1: procedure  $ALG_1(\varphi)$ 
2:    $\psi := f(\varphi)$ 
3:    $\rho := ALG_2(\psi)$ 
4:   return  $g(\rho)$ 

```

ALG_1 is *complete* (i.e., works on all inputs), since f, g and ALG_2 are. The remainder of the proof shows that ALG_2 is at most as rapid as ALG_1 , i.e., there exists a polynomial p such that for all operands $\psi \in D_2$, there exists in input $\varphi \in D_1$ with $|\varphi| = |\psi|$ for which $time(ALG_1, \varphi) \leq p(time(ALG_2, \psi))$.

Let $\psi \in D_2$. We take $\varphi \in D_1$ such that $|\varphi| = |\psi|$ and $|\varphi| \leq s(|\psi|)$ for the polynomial s ensuring the succinctness relation $D_1 \preceq_s D_2$. Such a φ exists, because D_1 is more succinct than D_2 .

It remains to show that $\exists p: time(ALG_1, \varphi) \leq p(time(ALG_2, \psi))$, where p is independent of φ and ψ . To this end, we can express the time required by ALG_1 by summing the runtimes of its three steps as follows.

$$time(ALG_1, \varphi) = time(f, \varphi) + time(ALG_2, f(\varphi)) + time(g, ALG_2(f(\varphi))) \quad (22)$$

It now suffices to prove that each summand of Eq. (22) is polynomial in the runtime of $ALG_2(\psi)$.

1. We show $time(f, \varphi) \leq \text{poly}(time(ALG_2, \psi))$. Since f runs in polynomial time in its output (A3) and $|\varphi| \leq s(|\psi|)$ (see above), we have $time(f, \varphi) \leq \text{poly}(|f(\varphi)|)$. Let t be the polynomial such that $time(f, \varphi) \leq t(|f(\varphi)|)$. Since f

is weakly minimizing (A3), it is guaranteed that $|f(\varphi)| \leq m(|\psi|)$ for some polynomial m . Lastly, by A1, we have $|\psi| = \mathcal{O}(\text{time}(\text{ALG}_2^m, \psi))$, so $|\psi| \leq k(\text{time}(\text{ALG}_2, \psi))$ for some polynomial k . Put together, we have $\text{time}(f, \varphi) \leq t(|f(\varphi)|) \leq t(m(|\psi|)) \leq t(m(k(\text{time}(\text{ALG}_2, \psi))))$, which proves the claim.

2. We show $\text{time}(\text{ALG}_2, f(\varphi)) \leq \text{poly}(\text{time}(\text{ALG}_2, \psi))$. Because f is a weakly minimizing transformation (A3), we have $|f(\varphi)| \leq s(|\psi|)$ for some s . Since ALG_2 is runtime monotonic (A2), and because $|f(\varphi)| \leq s(|\psi|)$, we have $\text{time}(\text{ALG}_2, f(\varphi)) \leq t(\text{ALG}_2, \psi)$ for some t , which proves the claim.
3. We show $\text{time}(g, \text{ALG}_2(f(\varphi))) \leq \text{poly}(\text{time}(\text{ALG}_2, \psi))$. Since g runs in time polynomial in the input (A4); and the input to g is $\text{ALG}_2(f(\varphi))$, we have $\text{time}(g, \text{ALG}_2(f(\varphi))) \leq p(|\text{ALG}_2(f(\varphi))|)$ for some polynomial p . Next, we have trivially $\text{time}(\text{ALG}_2, f(\varphi)) \geq |\text{ALG}_2(f(\varphi))|$, since the time ALG_2 spends writing the output is included in the total time, thus we obtain $\text{time}(g, \text{ALG}_2(f(\varphi))) \leq p(\text{time}(\text{ALG}_2, f(\varphi)))$. As we have seen above in item 2, $\text{time}(\text{ALG}_2, f(\varphi)) \leq t(\text{time}(\text{ALG}_2, \psi))$ for some polynomial t . Putting this together, we obtain $\text{time}(g, \text{ALG}_2(f(\varphi))) \leq p(t(\text{time}(\text{ALG}_2, \psi)))$, which proves the claim.

This proves the theorem for the case when OP is a manipulation operation.

Lastly, if OP is a query operation rather than a manipulation operation, then the transformation from D_2 back to D_1 using g is no longer necessary. This is the only change needed in ALG_1 ; in the proof above, we may use $\text{time}(g, \text{ALG}_2(f(x_1))) = 0$. The requirement that $\text{time}(g, \text{ALG}_2(f(x_1))) \leq p(\text{time}(\text{ALG}_2, x_2))$ now holds vacuously. \square

D.3 Rapidity Relation between Data Structures

Here we prove the rapidity relations between data structures studied in the paper as stated in Th. 6, restated below with proof.

Theorem 6. The rapidity relations in Fig. 9 hold.

Proof. The relation between SLDD_\times and MPS is proved in Th. 7 as restated in App. D.4. Finally, App. D.5 provides the transformations between QDDs that fulfill the conditions of Th. 5. \square

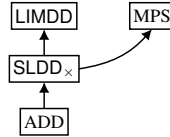


Figure 9: Rapidity relations between data structures considered here. A solid arrow $D_1 \rightarrow D_2$ means D_2 is at least as rapid as D_1 for all operations satisfying A1 and A2 of Th. 5.

D.4 MPS is at least as Rapid as SLDD_\times

This appendix proves Th. 7 from Sec. 5.2 by providing transformations between MPS and SLDD_\times that realize the sufficient conditions of Th. 5. The introduction into QDDs, given in App. A.2 is relevant here.

Theorem 7. MPS is at least as rapid as SLDD_\times for all operations satisfying A1 and A2.

Proof. Let f be the polynomial-time transformation from Lem. 39. Let g be the weakly minimizing transformation from MPS to SLDD_\times of Lem. 40, that runs in time polynomial in the size of the input MPS and the resulting SLDD_\times . These transitions satisfy requirements A3 and A4 of Th. 5 respectively. Since QDDs are canonical data structures as explained in Sec. 2, all algorithms are by definition runtime monotonic, as for any state $|\varphi\rangle$ there is only one structure representing it, i.e., D^φ is a singleton set. This satisfies A2. Since its premise fulfills A1, the theorem follows. \square

Lemma 39 (SLDD $_\times$ to MPS). In polynomial time, a SLDD_\times can be converted to an MPS representing the same state.

Proof. Consider a SLDD_\times with root edge $\xrightarrow{\lambda} \textcircled{v}$ describing a state $|\varphi\rangle = \sum_{\vec{x} \in \{0,1\}^n} \alpha(\vec{x}) |\vec{x}\rangle$. We will construct an MPS A describing the same state. For the purposes of this proof, we will call low edges 0 -edges and high edge 1 -edges.

First, without loss of generality, we may assume that the root edge label is $\lambda = 1$. Namely, we may multiply the labels on the root's low and high edges with λ , and then set the root edge label to 1; this operation preserves the state represented by the SLDD_\times .

Denote by D_ℓ the number of nodes at the ℓ -th layer in $\text{SLDD}_\times v$, i.e. $D_n = 1$ (the root node v) and $D_0 = 1$ (the leaf $\boxed{1}$). Recall that the SLDD_\times is a directed, weighted graph whose vertices are divided into $n + 1$ layers, i.e., the edges only connect nodes from consecutive layers. Therefore, we may speak of the $D_\ell \times D_{\ell-1}$ bipartite adjacency matrix between layer ℓ and layer $\ell - 1$ of the diagram. For layer $1 \leq \ell \leq n$ and $x = 0, 1$, let A_ℓ^x be the $D_\ell \times D_{\ell-1}$ bipartite adjacency matrix obtained in this way using only the low edges if $x = 0$, and only the high edges if $x = 1$. That is, assuming some order on nodes within each level, the entry of the matrix A_ℓ^x in row r and column c is defined as

$$(A_\ell^x)_{r,c} = \begin{cases} \text{label}(e) & \text{if node with index } r \text{ in level } \ell \text{ has a } x\text{-edge } e \text{ to node with index } c \text{ in level } \ell - 1 \\ 0 & \text{otherwise} \end{cases} \quad (23)$$

We claim that the following MPS A describes the same state as the SLDD_\times :

$$A = (A_1^0, A_1^1, \dots, A_n^0, A_n^1) \quad (24)$$

Following the MPS definition in Sec. 2, our claim is proven by showing that for SLDD_\times root node v representing $|v\rangle$, we have

$$\langle \vec{x} | v \rangle = A_n^{x_n} \cdot A_{n-1}^{x_{n-1}} \cdots A_1^{x_1} \quad \text{for all } \vec{x} \in \{0, 1\}^n \quad (25)$$

For an n -qubit $\text{SLDD}_\times v$, the amplitude $\langle \vec{x} | v \rangle$ for $\vec{x} \in \{0, 1\}^n$ is equal to the product of the weights found on the single path from the root node to leaf effected by \vec{x} (this path is found as follows: go down from root to leaf; at a vertex at layer j , choose to traverse the low edge if $x_j = 0$ and the high edge if $x_j = 1$). We next reason that this product equals the single entry of the product $y := A_n^{x_n} \cdot A_{n-1}^{x_{n-1}} \cdots A_1^{x_1}$ from Eq. (25).

We recall several useful facts from graph theory. If G (G') is a weighted, directed bipartite graph on the bipartition $M \cup M''$ ($M'' \cup M'$) vertices, with weighted adjacency matrix A_G ($A_{G'}$), then it is not hard to see that the element $(A_G \cdot A_{G'})_{r,c}$ is the sum, over all two-step paths $r-a-c$ starting at vertex $r \in M$ and going through vertex $a \in M''$ to vertex $c \in M'$, of products of the two weights $w_{r \rightarrow a}$ and $w_{a \rightarrow c}$. More generally, for a sequence of weighted, directed bipartite graphs G_j with vertex set $M_j \cup M_{j+1}$, the (r, c) -th entry of the product of adjacency matrices $A_{G_1} \cdot A_{G_2} \cdots A_{G_n}$ equals $\sum_{\text{paths } \pi \text{ from } r \text{ to } c} \prod_{\text{edge } e \in \pi} \text{weight}(e)$.

Now note that the matrix y has dimensions 1×1 (since $D_0 = D_n = 1$), corresponding to a single root and single leaf. By the reasoning above, since y is the product of all bipartite adjacency matrices of the SLDD_\times , the single element of this matrix is equal to the product of weights found on the single path from root to leaf as represented by \vec{x} . \square

Lemma 40 (MPS to SLDD_\times). There is a weakly minimizing transformation from MPS to SLDD_\times , that runs in time polynomial in the size of the input MPS and the resulting SLDD_\times .

Proof. Alg. 4 shows the algorithm which converts an MPS to a SLDD_\times . The idea is to use perform backtracking to construct the SLDD_\times bottom-up. Specifically, given an MPS $\{A_n^0, A_n^1, \dots, A_1^0, A_1^1\}$ representing a state $|\varphi\rangle = |0\rangle|\varphi_0\rangle + |1\rangle|\varphi_1\rangle$, the MPS for $|\varphi_0\rangle$ is easily constructed by setting the first open index to 0 and contracting these two blocks, i.e., $A_{n-1}^0 := A_n^0 \cdot A_{n-1}^0$ and $A_{n-1}^1 := A_n^0 \cdot A_{n-1}^1$, and similarly for $|\varphi_1\rangle$. We then recurse, constructing MPS for states $|\varphi_{00}\rangle, |\varphi_{01}\rangle$, etc. When we find a state whose SLDD_\times node we have already constructed, then we may simply return an edge to that SLDD_\times node without recursing further. This dynamic programming behavior is implemented through the check at line 3.

Through the use of dynamic programming with the cache set D , it is clear that the number of recursive calls to MPS2SLDD_\times is bound by the number of edges in the resulting SLDD_\times . Dynamic programming is implemented by checking, for each call with MPS M , whether some SLDD_\times node $v \in D$ already represents $|M\rangle$ up to a complex factor. To this end, the subroutine `EQUIVALENT`, on line 3, checks whether $|M\rangle = \lambda \cdot |v\rangle$ for some $\lambda \in \mathbb{C}$. It is straightforward to see that it runs in polynomial time in the sizes of $\text{SLDD}_\times v$ and MPS M : first, it creates an MPS for the given SLDD_\times node v using the efficient transformation in App. D.4. Next, it computes several inner products on MPS, which can also be done in polynomial time, using the results in App. C. This `EQUIVALENT` operation is called $|D|$ time, which dominates the runtime of each call MPS2SLDD_\times . Therefore the entire runtime is polynomial in the sizes of the MPS and the resulting SLDD_\times .

Since SLDD_\times is canonical, the transformation is weakly minimizing by definition. \square

Algorithm 4: An algorithm which converts an MPS into a SLDD_\times . It runs in time polynomial in $s + d$, where s is the size of the SLDD_\times , and d is the bond dimension of the MPS. Here D is the diagram representing the state. The subroutine $\text{EQUIVALENT}(v, M)$ computes whether the vectors $|v\rangle, |M\rangle$ are co-linear, i.e., whether there exists $\lambda \in \mathbb{C}$ such that $|M\rangle = \lambda |v\rangle$.

```

1:  $D := \{\textcircled{1}\}$  ▷ Initiate diagram  $D$  with only a  $\text{SLDD}_\times$  leaf node representing 1
2: procedure  $\text{MPS2SLDD}_\times(\text{MPS } M = \{A_j^x\})$  ▷ Returns a root edge  $e_R$  such that  $|e_R\rangle = |M\rangle$ 
3:   if  $D$  contains a node  $v$  with  $|M\rangle = \lambda |v\rangle$  then return  $\xrightarrow{\lambda} \textcircled{v}$  ▷ Implemented with  $\text{EQUIVALENT}(v, M)$  for all  $v \in D$ 
4:    $\text{EDGE } e_0 := \text{MPS2SLDD}_\times(\{A_n^0 \cdot A_{n-1}^0, A_n^0 \cdot A_{n-1}^1\} \cup \{A_{n-2}^0, A_{n-2}^1, \dots, A_1^0, A_1^1\})$ 
5:    $\text{EDGE } e_1 := \text{MPS2SLDD}_\times(\{A_n^1 \cdot A_{n-1}^0, A_n^1 \cdot A_{n-1}^1\} \cup \{A_{n-2}^0, A_{n-2}^1, \dots, A_1^0, A_1^1\})$ 
6:    $\text{NODE } w := \textcircled{x} \xrightarrow{e_0} \dots \textcircled{y} \xrightarrow{e_1} \textcircled{w}$  ▷ Create new node  $w$  with  $\text{MAKENODE}$ 
7:    $D := D \cup \{w\}$ 
8:   return  $\text{EDGE } \xrightarrow{1} \textcircled{w}$ 

9: procedure  $\text{EQUIVALENT}(\text{SLDD}_\times \text{ NODE } v, \text{MPS } M = \{A_j^x\})$ 
10:   $V := \text{SLDD}_\times 2\text{MPS}(v)$  ▷ Using transformation in App. D.4
11:   $s_V := \sqrt{|\langle V|V \rangle|}$  ▷ Compute inner product
12:   $s_M := \sqrt{|\langle M|M \rangle|}$  ▷ Compute inner product
13:   $\lambda := 1/s_V \cdot s_M \langle V|M \rangle$  ▷ Compute inner product
14:  if  $|\lambda| = 1$  then return " $|M\rangle = \frac{s_M}{s_V} \lambda |v\rangle$ "
15:  else return " $|v\rangle$  is not equivalent to  $|M\rangle$ "

```

Algorithm 5: An algorithm which converts a LIMDD into an SLDD_\times .

```

1:  $\text{SLDD}_\times D := \{\xrightarrow{1} \textcircled{1}\}$  ▷ The  $\text{SLDD}_\times$  is initialized to contain only the Leaf
2: procedure  $\text{LIMDD 2SLDD}_\times(\text{LIMDD edge } \xrightarrow{\lambda P_n \otimes P'} \textcircled{v})$ 
   Returns (a pointer to) an edge to a  $\text{SLDD}_\times$  node
3:   if  $v$  is the Leaf node then return  $\xrightarrow{\lambda} \textcircled{v}$ 
4:    $R := \text{GETLEXMINLABEL}(P_n \otimes P', v)$ 
5:   if the  $\text{CACHE}$  contains tuple  $(R, v)$  then return  $\lambda \cdot \text{CACHE}[R, v]$ 
6:   for  $x = 0, 1$  do
7:      $\text{SLDD}_\times \text{ edge } r_x := \text{FOLLOW}_x(\xrightarrow{P_n \otimes P'} \textcircled{v})$ 
8:      $\text{SLDD}_\times \text{ edge } r := \text{MAKEEDGE}(r_0, r_1)$ 
9:      $\text{CACHE}[R, v] := r$ 
10:     $D := D \cup \{r\}$  ▷ Add the new edge to the diagram
11:    return  $\lambda \cdot r$ 

```

D.5 Transformations between QDDs

QDDs are canonical data structures as explained in Sec. 2. Therefore, (i) all algorithms are by definition runtime monotonic, as for any state $|\varphi\rangle$ there is only one structure representing it, i.e., D^φ is a singleton set; and (ii) all transformations given below are therefore weakly minimizing since they convert to a canonical data structure (namely, since they map to the unique element in D^φ , in particular they map to the minimum-size element of D^φ).

LIMDD to SLDD_\times Alg. 5 converts a LIMDD to a SLDD_\times in time linear in the size of the output. The diagram is the set of edges D , which is initialized to contain the Leaf (i.e., the node $\xrightarrow{1} \textcircled{1}$), and is filled with the other edges during the recursive calls to $\text{LIMDD 2SLDD}_\times$. The function GETLEXMINLABEL is taken from Vinkhuijzen et al. (Vinkhuijzen et al. 2023a); it returns a canonical edge label.

SLDD_\times to LIMDD By definition, a SLDD_\times can be seen as a LIMDD in which every edge is labeled with a complex number and the n -qubit identity tensor $\mathbb{I}^{\otimes n}$. Thus, a transformation does not need to do anything. Optionally, it is possible to convert a given LIMDD to one of minimum size, as described by (Vinkhuijzen et al. 2023a).

ADD to SLDD_x To convert an ADD into a SLDD_x, we add a Leaf node labelled with 1; then, for each Leaf node labelled with $\lambda \neq 1$, we label each incoming edge with λ , and then reroute this edge to the (new) Leaf node labelled with 1. Optionally, the resulting SLDD_x can be minimized to obtain the canonical instance for this state, using, e.g., techniques from (Miller and Thornton 2006; Brace, Rudell, and Bryant 1990).

SLDD_x to ADD Alg. 6 gives a method which converts an SLDD_x to an ADD. It is very similar to the ones used in the transformation LIMDD to SLDD_x above, . We here check whether the diagram already contains a function which is pointwise equal to the one we are currently considering. If so, we reuse that node; otherwise, we recurse.

Algorithm 6: An algorithm which converts an SLDD_x to an ADD. Its input it an SLDD_x edge e representing a state $|e\rangle$ on n qubits. Here the method FOLLOW_x(e) returns an SLDD_x edge representing the state $\langle x | \otimes \mathbb{I}^{\otimes n-1} \cdot |e\rangle$. It outputs an SLDD_x node w representing $|w\rangle = |e\rangle$.

```

1: procedure SLDDx 2ADD(SLDDx edge  $e = \xrightarrow{\lambda} \textcircled{v}$  on  $n$  qubits)
2:   if  $n = 0$  then
3:      $w := \xrightarrow{\lambda} \textcircled{\lambda}$ 
4:   else if  $A$  contains a node  $w$  with  $|v\rangle = |w\rangle$  then
5:     return  $w$ 
6:   else
7:     for  $x = 0, 1$  do
8:        $w_x := \text{SLDD2ADD}(\text{FOLLOW}_x(e))$ 
9:       SLDDx Node  $w := \textcircled{w_0} \dots \textcircled{w_1}$ 
10:     $A := A \cup \{w\}$ 
11:    return  $w$ 

```
